A THESIS

On

Magicity Among Super Deformed Nuclei using Two Center Shell Model

Submitted in the partial fulfillment of requirement for the award of the Degree of

Master of Science (PHYSICS)

Submitted by: **Shilpy Singla**

Roll No.: 30704017

Under the Guidance of

Dr. Manoj Kumar Sharma

(Assistant Professor**)**

School of Physics and Materials Science

THAPAR UNIVERSITY

PATIALA (PUNJAB)-147 004

JUNE 2009

CERTIFICATE

This is to certify that the report entitled "**Magicity Among Super Deformed Nuclei using Two Center Shell Model**" submitted by **Shilpy Singla, Roll No. 30704017,** student of M.Sc. (Physics), Thapar University, Patiala, was carried out by her under my supervision. She has not submitted this material for credit towards any other degree at Thapar University, Patiala or at any other university.

13/7/09

(Dr. Manoj. K. Sharma)
Assistant Professor
School of Physics & Materials Science
Thapar University Patiala

13/7/09

(Dr. O. P. Pandey)
Professor and Head
School of Physics &
Materials Science
Thapar University Patiala

13/7/09

(Dr. R. K. Sharma)
Dean of Academic Affairs
Thapar University
Patiala

Dedicated to:

God who gave me life

And

My Lovable Parents who made it worth living

ACKNOWLEDGEMENTS

I would have never succeeded in completing my task without the cooperation, encouragement and help provided to me by various personalities. I express my deep sense of gratitude and respect to my guide **Dr. Manoj K. Sharma, Assistant Professor, School of Physics and Material Science, Thapar University, Patiala,** for his keen interest and valuable guidance, strong motivation and constant encouragement during the course of the work. I thank him from the bottom of my heart for introducing me to Nuclear Physics, for his great patience, constructive criticism and myriad useful suggestions apart from invaluable guidance to me. I am sure that the knowledge gained through my association with my supervisor shall go a long way in helping me to realize my goals in life.

My sincere thanks also goes to Dr. O. P. Pandey, Professor and Head School of Physics and Materials Science, Thapar University, Patiala, for providing all the necessary facilities in the department. I also wish to thank all the faculty and staff of the School of Physics and Material Science for their kind support.

My special thanks to Mrs. Shefali Kanwar, Dr. BirBikram Singh and all the Research Scholars, for their timely help, cooperation and good wishes at various stages of my thesis work. I am also thankful to my all classmates for their help and support at every stage during the thesis work.

Last but not the least, I would like to thank my family, without whom I am nothing, to provide me great opportunities, everlasting support, big encouragement and lots of love.

Shilpy Singla

(MS.SHILPY SINGLA)

Abstract

The relative stability of superdeformed nuclei in mass region A=68-82 has been carried out systematically in the recent times on the basis of cluster decay process. These studies establish that ^{76}Kr is the most stable nucleus among various isotopes of Sr and Zr isotopes in this special island of superdeformed nuclei. These studies are extremely important in order to understand various nuclear properties and synthesis process of heavy/superheavy nuclear systems. It is relevant to mention here that deformed /superdeformed target projectile combinations are being preferred in recent times for the obvious reason that the fusion probability gets enhanced with the choice of target/projectile combinations in place of spherical ones, in the present work we have carried out systematic study and the decay of stable nucleus ^{76}Kr using Two Center Shell Model (TCSM). We have done the calculations for four nucleon clusterization of ^{76}Kr. Here we have optimized the quadrupole deformation (β_{21}) of one fragment and vary the β_{22} of the complementary fragment. The gap between last filled and first empty level gets maximized. The λ (elongation) is taken at touching configuration and ε (neck parameter) is taken fix as ε=0.75 as referred to dinuclear system model calculations. Our TCSM, calculations clearly depict that ^{76}Kr nuclear system is most stable against ^{16}O cluster followed by fragment mass A_2 =32, 36 and 20.

CONTENTS

List of figures

Chapter 1

INTRODUCTION

Introduction:-

The branch of physics concerned with studying and understanding the atomic nucleus, including its composition and the forces which bind it together, is called nuclear physics.As the name implies, nuclear physics is the study of the nuclei which lie at the core of every atom in the world. Over 99.9% of the mass of all the ordinary matter in the universe is found in nuclei. Protons and neutrons are the building blocks of the nucleus, so a large part of nuclear physics is trying to understand the force that holds protons and neutrons together.

The periodic table of the elements is slowly getting bigger. At one time it contained only 92 (83 naturally occurring and stable elements and 9 radioactive elements), starting with hydrogen and ending with uranium (Z=92). Majority of these elements have half-lives that are comparable to the age of the Earth, which is about 4.5 billion years old. Since 1940s, however, physicists have been able to produce unstable elements that decay to lighter elements on timescales that can range from thousands of years to tiny fractions of a second. There is, however, more to this branch of physics than simply creating heavier and heavier elements. It is also essential to understand the behaviour of these new elements, many of which do not yet have official names.

1.1 Super Heavy elements:-

A heavy element is an element with an atomic number greater than 92. The first heavy element is neptunium (Np), which has an atomic number of 93 and the term Super Heavy Elements to refer to those elements with an atomic number greater than or equal to 112. The first super heavy element is element 113. Like some of the heavy elements, superheavy elements are produced artificially in cyclotron experiments. The formation of super and highly deformed rotating nuclei as well as superheavy elements is possible only via fusion reactions and

the potential barriers encountered by the nuclear system in the entrance channel play a main role. In this path the saddle-point corresponds to two separated but close nuclei maintained in unstable equilibrium by the balance between the attractive nuclear proximity forces and the repulsive Coulomb forces. Later on, a bridge of matter takes form between the two still almost spherical nuclei. Finally the nuclear system undergoes fusion, quasi-fission or fission while emitting some nucleons.

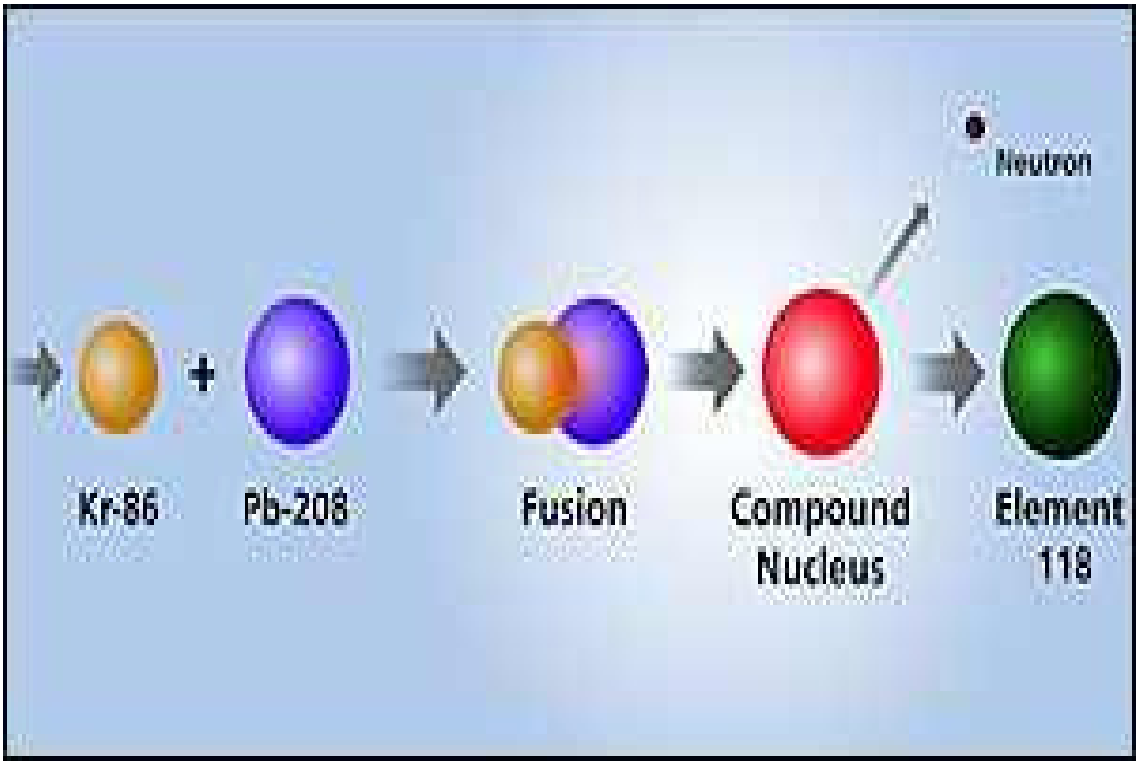

Figure.1.1: Synthesis of Super Heavy Eements

Superheavy elements allow nuclear physicists to explore concepts such as "magic numbers" and the "island of stability", which help us understand why some nuclei are more stable than others. They can also be used to test the predictions of different models of the nucleus and, ultimately, they may help us to understand why nature contains only a finite number of elements. By last year a total 114 elements were known, and earlier this year the author and co-workers reported the synthesis of two new "superheavy" elements.There are 92 elements that are found in nature. Out of these 92 elements, elements up to charge

number 83 are stable and they last forever. Elements having an atomic number greater than 83 are radioactive (Po, At, Rn, Fr, Ra, Ac, Th, Pa, U), but their decay is so slow that they are still around. Thus, these 92 elements are the stable continent that we use and live by. Since the 1940s, however, physicists have been able to produce unstable elements that decay to lighter elements on timescales that can range from thousands of years to tiny fractions of a second

The "island of stability" refers to a predicted region of super heavy elements on the chart of nuclides with half-lives that are longer by several orders of magnitude than the half-lives of other super heavy elements. Half-lives for elements in the island of stability may range from seconds to minutes, while half-lives for other super heavy elements may be measured in micro- or nanoseconds. The existence of the island of stability was shown in 1998 with the discovery of the super heavy element 114. The chart of the nuclides, showing all nuclides that have at some time been observed experimentally as a function of their proton number Z and neutron number N. On this chart of the nuclides (isotopes), black squares represent stable nuclei and the yellow squares indicate unstable nuclei that have been produced and studied in the laboratory. The many thousands of these unstable nuclei yet to be explored are indicated in green. The red vertical and horizontal lines show the magic numbers, reflecting regions where nuclei are expected to be more tightly bound and have longer half-lives.The island of stability (Fig.1.2) is a specific subset of the super heavy elements, which is characterized by nuclei that have a spherical shape. From the plot it is evident that for the light nuclei (A < 20) have n/p ratio is close to unity, for heavy nuclei (A > 20) the n/p ratio increases progressively due to dominance of number of neutrons. Thus stable nuclei (non-radioactive) have n/p ratio between 1 - 1.6. These lie in the shaded region of the plot which is also called stability belt or stability zone. The elements whose nuclei do not fall within the stability zone are said to be unstable. The unstable nuclei, whose n/p ratio is either less than 1 or greater than 1.6, disintegrate giving out α, β, γ rays in their attempt to attain stability. The process of disintegration continues till the n/p ratio falls within the stability limit

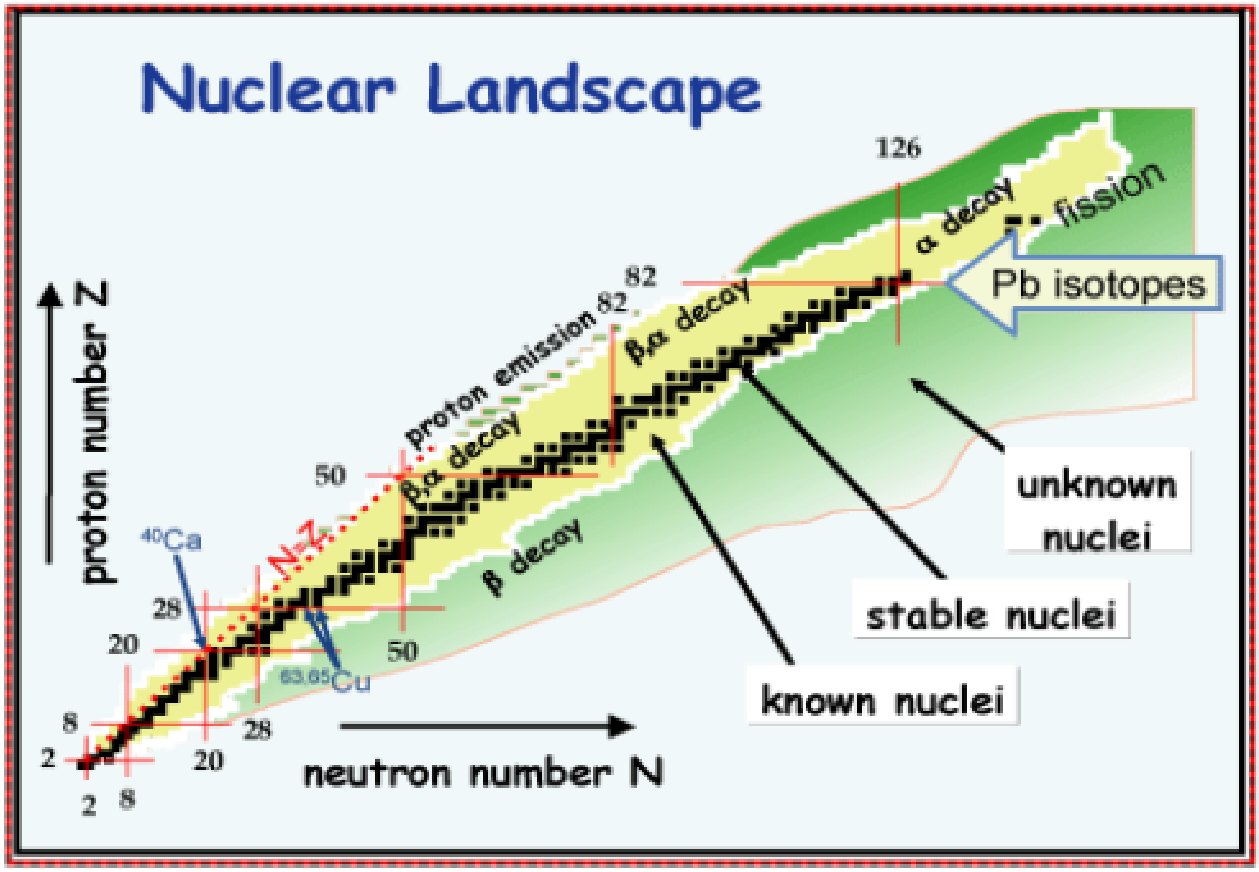

Figure.1.2: Island of Stability

Since then, the question whether the island of stability exists for these super heavy nuclei and where the border of such an island may lie, has been one of the most fascinating and elusive open question in modern physics. Very intensive theoretical and experimental studies are being made to find an answer to this problem in different scientific centers of the world. This research for super heavy elements (Z > 100) explores the borderline of the nuclear chart towards its upper end where the strong Coulomb force acting between the many protons dominates the nuclear stability and finally terminates the number of elements by instability against fission. These discoveries will help physicist to understand as to how nuclei are held together and how they resist fission. They can also be

used to test the predictions of different models of the nucleus and, ultimately, may help us to understand why nature contains only a finite number of elements. The study of these elements provides an excellent possibility regarding the understanding of nuclear structure in a strong Coulomb field. Theoretically, various models have been developed for the study of super-heavy elements (SHEs). The first realistic theoretical calculations for the super-heavy nuclei were carried out in 1966. These early calculations were based on Struntinsky [1] macro-microscopic method that superimposes the shell strength as a correction to deformed liquid drop energy. Its main assumption is that the total energy of a nucleus can be decomposed in two parts, $E = E_{macro} + E_{micro,}$ where E_{macro} is the macroscopic liquid drop energy and E_{micro} is the microscopic energy calculated from a non-self consistent average potential.

In other words, the total binding energy is decomposed into a smooth part (approximated by a macroscopic liquid drop model) and a microscopic quantum shell correction term strongly oscillating with the number of nucleons and reflecting the energy stabilization due to the presence of nucleonic shells. Using this method, Myers and Swiatecki [2], Nilsson et al. [3, 4], Mosel and Griener [5], Fizet and Nix [6] and Randrup et al. [7] made a wide range of studies for the super-heavy mass region. Such calculations predicted the nucleus with Z=114, N=184 to be a doubly magic center of an island of long lived super-heavy nuclei.

The challenge presented to experimental nuclear physicists is clear: they need to create the super-heavy nuclei and measure their properties to put these theoretical predictions to the test. Hunting the SHEs is not an easy task. Production of SHEs is quite tedious, as the increase in the charge of a nucleus makes it increasingly unstable against fission. Untiring searches over decades have now reached the point where new SHEs have been synthesized at various labs. in Darmstadt (GSI), Berkley and Dubna and finally they have succeeded in jumping over the sea of instability on to an island of stability, at least in protons, that theories have been predicting since the late 1960s. Note that in first transuranium elements, synthesized in successive neutron-capture reactions at the Lawrence Berkeley Laboratory between 1940 and 1953, the nuclei gain extra

neutrons during long exposures in a high-neutron-flux reactor, which resulted in the discovery of new elements with atomic numbers up to 100 (Fermium). However, super-heavy nuclei could not be explored with this technique because they decay before capturing the available extra neutron. In an effort to produce elements heavier than Fermium, researchers turned to heavy-ion reactions, in which two nuclei, one a heavy-ion beam the other a target nucleus are forced to undergo a fusion reaction to create a heavier compound nucleus. Heavy-ion reactions are a very fast developing subject of nuclear physics and carries immense potential to address various unresolved issues related to nuclear reaction dynamics.

The trouble with this approach, however, is that the collisions between the ions leave the resulting compound nucleus in a highly excited state, which means that it is more likely to undergo fission or some other competing process immediately after its formation. It is a well reported aspect that fusion probability enhances with the incorporation of deformation and orientation effects. That is certain heavy / super heavy elements have been synthesized with the deformed target projectile combinations with a reasonable success. It is therefore believed that a proper choice of deformed target/ projectile could give a suitable combination for the synthesis of these heavier nuclear systems.

1.2 **Deformed and Superdeformed Nuclei**:-

Nuclei can be both spherical and deformed in their ground state. The shape of both nuclei participating in a reaction affects the barrier height and the potential of their interaction. The barrier height is of great importance for the reactions of sub barrier fusion and synthesis of superheavy elements. Nuclear reactions, where deformed nuclei are engaged, are widely applied to the synthesis of superheavy elements in many laboratories around the world. The reactions of sub barrier fusion of strongly deformed F, Ne, and Mg isotopes play a very important role in the burning of stars and govern their evolution. Therefore, it is important to study the properties of the interaction potential between two

deformed nuclei. Beside this proper choice of orientation of target and projectile contribute immensely and therefore need to be handled with care. In other words; where ever a deformed configuration is considered. One can not ignore the orientation behavior of nuclear systems. The spherical, oblate and prolate shapes of a nuclear system are shown in Fig 1.3

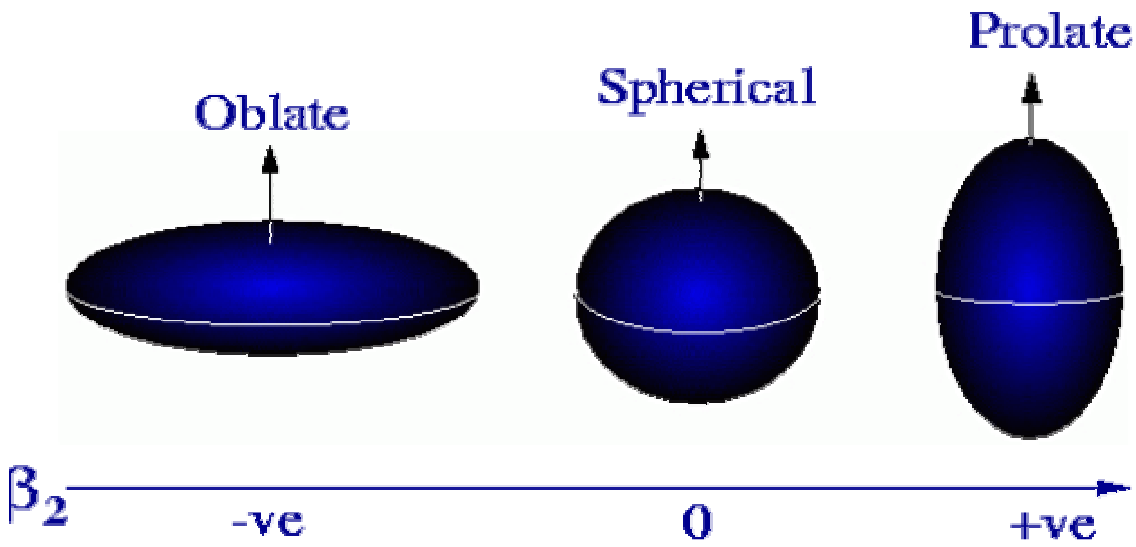

Figure.1.3: Nuclear Shapes for oblate, spherical and prolate nucleus

Nuclei are considered to be super deformed when the nucleus acquires an elongated shape that can be represented as an approximate ellipsoid where the ratio of the long to short axis is considerably larger. These super deformed nuclei can undergo spontaneous fission. At high spin rotation, some nuclei are found to be stable, having an axial deformation corresponding to a major-to-minor axis ratio of 2:1. Nuclei stable against this extra-ordinary deformation are named super deformed nuclei. These nuclei have a very large quadrupole moment and their rotational frequencies are extremely large; for energy of 0.6 MeV, the corresponding rotational frequency is 1022Hz. Since its discovery in 1985 as a secondary minimum to a fission potential barrier, super deformation has become a very active field of research in both experimentally and theoretically nuclear physics. So far, more than 300 rotational bands related to

the rotation of super deformed nuclei have been observed and studied in many regions across the nuclear mass range.

1.3 Importance of Super Deformed Nuclei:-

The depth and the width of the capture well in the nucleus-nucleus interaction potential, as well as the barrier height are known to play a dominant role in the formation of a compound nucleus in fusion-fission reaction. This feature is associated with the necessity to overcome the barrier that exists between two separated nuclei and with a formation of a scission neck between contacting nuclei in the capture well, as well as with the following evolution of shape of the nuclear system. Therefore, it is very important to study the influence of deformation and an orientation on the nucleus-nucleus interaction potential. The fission of an atomic nucleus is a unique process in which a nuclear collective motion sets in involving all nucleons in the nucleus and a large number of nucleons are eventually transported across the fission barrier. A nucleus splits into two fragments during fission process and exhibit variety of shapes while transporting from equilibrium configuration to that of scission configuration. The instant at which the elongated heavy nucleus breaks into separate pieces is called the scission point.

A quadruple deformation can give rise to two kinds of shape distributions:

1) It can cause a prolate deformation, making the spherical nucleus actually appear more like a football, positive quadrupole deformations.
2) It can cause an oblate deformation, making the spherical nucleus actually appear more like a doorknob, negative quadrupole deformations.

It has been observed that when we opt for a deformed target/ Projectile combination for the synthesis of heavy/ superheavy nuclei the fusion probability in general increased quite significantly.

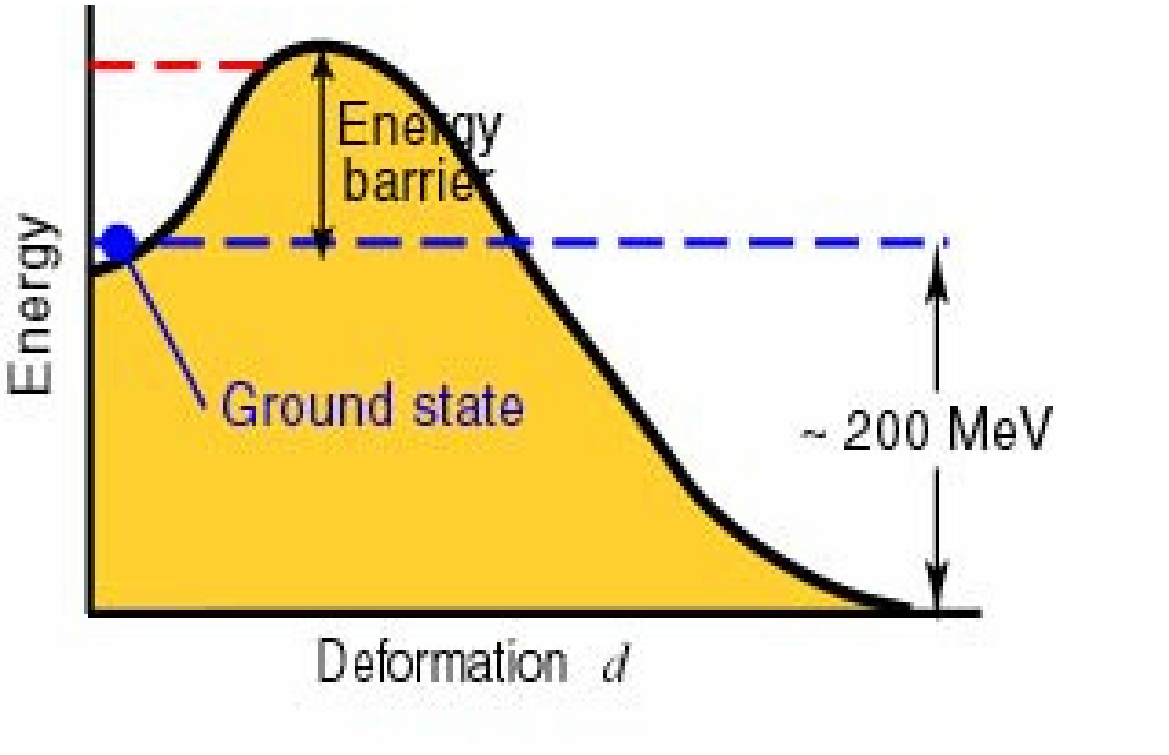

Figure.1.4 Potential Barrier vs. deformation

The apparent reason for this enhancement in fusion probability is that when we take a deformed reaction partner the fusion barrier becomes shallow and gets distributed to provide easier path for compound nucleus formation.

Several experimental techniques have been used to make new elements. Some of these include heavy ion transfer reactions, cold or hot fusion evaporation reactions, neutron capture reactions, light-ion charged particle induced reactions, and even nuclear explosions. These techniques each have advantages and disadvantages making them suitable for studying nuclei in certain regions. The types of nuclear reactions that have been successfully used to produce new elements in the last decade are cold fusion reactions and hot fusion reactions.

Broadly speaking, a super heavy element can be synthesized by taking hot or cold fusion interaction criteria.

1.4 Cold Fusion Reactions:-

Cold fusion reactions using targets/beams of ^{208}Pb and ^{209}Bi and projectiles/targets of the most neutron rich isotopes of the even Z elements from Ca to Zn succeeded in extending the periodic table of elements from Z = 102 to Z = 112. Theoretically, "Cold fusion" reactions correspond to lowest interaction barriers, largest interaction radii and non-compact, elongated nuclear shapes, with the excitation energy of the compound nucleus formed to lie between 10-20 MeV. These reactions are weakly exothermic reactions. At excitation energies of 10-20 MeV, 1-2 neutrons are emitted from the compound nucleus. Cold synthesis of SHEs was first proposed theoretically by Greiner, Gupta and collaborators at Frankfurt [25-26] as early as in 1974-75, more than three decades back, on the basis of Quantum Mechanical Fragmentation Theory using the Two center shell model as an average two-body potential within the Strutinsky macro-microscopic method. They suggested the use of cold compound systems that were formed for all target-projectiles systems that lie at the bottom of the potential energy minima.

Four such reaction valleys were always found to exist, namely with:

- Symmetric or nearly symmetric nuclei,
- Asymmetric nuclei with one or both deformed nuclei,
- Very asymmetric nuclei with Pb nucleus (or the neighboring Bi nucleus for odd Z compound systems) always as one of the reaction partners, and,
- Super-asymmetric target-projectiles (such as C, N, O and Ne) and heavy deformed targets.

The excitation energy is lowest for the case (i) of symmetric target-projectile combinations, but the above information on reaction valleys, when optimized by the requirements of cold fusion reactions (smallest interaction barrier, largest interaction radius and non necked nuclear shapes), singled out the use of of the reaction partners of case (iii) above, i.e. Pb (or Bi) as one of the reaction partners

always, for the cold synthesis of super heavy elements. Experimentally, however, it became possible to identify the true signatures of cold fusion phenomenon only in late 1990's. Most of the heaviest elements were produced in three heavy element research laboratories: Lawrence Berkeley Laboratory in Berkeley (USA), Joint Institute for Nuclear Research in Dubna (Russia) near Darmstadt (Germany). Cold fusion reactions were first studied at the cyclotrons U300 and U400 in Dubna using beams of isotopes from Ca to Cr [37]. However these experiments did not go beyond Sg (Z=106). With the development of accelerator facilities and detection techniques, in a series of experiments from 1981- 1984, the elements Bh (Z =107), Hs (Z =108) and Mt (Z =109) were synthesized at GSI Darmstadt, using cold fusion reactions. The lowest cross-section measured was 16 pb for one atom of ^{266}Mt.

During the following years, the sensitivity was increased to a detection level of one atom per week at a cross-section of 1 pb. Using the improved set up and different incident energies both below and above the barrier, synthesis of new elements Z = 110, 111 and 112 was successfully completed [38]-[43]. These experiments took place in the years 1994-1996. All earlier experiments, both at Dubna and Darmstadt, synthesizing the transactinides (Z > 103), were made either at one incident energy or at incident energies above the barrier. The reactions with beams of ^{70}Zn, ^{76}Ge, ^{82}Se and ^{86}Kr and targets of ^{208}Pb and ^{209}Bi investigated in recent years at GSI (for Z=113,116,118), GANIL (114,118), RIKEN (113,118), and LBNL (118) resulted in negative results with cross-section limits of about 0.5 to 1 pb.

1.5 Warm/Hot and very Hot Fusion Reactions:-

For the synthesis of heavy/superheavy nuclei using hot fusion reactions more asymmetric beam and target partners were used to produce a compound nucleus with generally higher excitation energy that typically requires evaporation of three to five neutrons, generate more neutron-rich isotopes of an element,

have lower survival probabilities with respect to fission, but have higher fusion probabilities.

An example of this type of reaction is

$$^{48}Ca + ^{244}Pu \rightarrow ^{288}114 + ^{4}n \qquad \text{---(1.1)}$$

(With a cross-section of ~1 Pico barn.)

Because of the neutron-richness of this isotope of element 114, it never subsequently decays to any known isotope, and thus its identification is more problematic.

Theoretically these fusion reactions are characterized by the largest interaction barriers, smallest interaction radii and compact nuclear shapes. For warm fusion reactions, commonly called hot fusion reactions, the compound nucleus excitation energy is around 30- 35 MeV and for the very hot fusion reactions it is 40-50 MeV. Compound nucleus de-excites with the emission of 3-4 neutrons for hot and ≥ 4 for very hot fusion reactions. These reactions were also explained on the basis of Quantum Mechanical Fragmentation Theory (QMFT).

On the other hand cold fusion reactions use beam and target nuclei that are closer to each other in mass in order to produce a compound nucleus (the complete fusion of one target nucleus with one beam nucleus) with generally lower excitation energy that typically requires evaporation of one or no neutrons. This generates fewer neutron-rich isotopes of an element that have higher survival probabilities with respect to fission, but have lower fusion probabilities.

An example of this type of reaction is

$$^{70}Zn + ^{208}Pb \rightarrow ^{277}112 + ^{1}n \qquad \text{---(1.2)}$$

with a cross-section of ~1 Pico barn.

Because the 112 isotope ultimately decays by α emission to known nuclei [namely isotopes of elements 102 (No) and 104 (Rf)], identification of this element is straightforward. The difference between cold and hot fusion reactions is not only a result from gradually different values of excitation energy, but there exists a qualitative difference, which on one hand (cold fusion) is based on a well

ordered fusion process along paths of minimum dissipation of energy, and on the other hand (hot fusion) is based on a process governed by the formation of a more or less equilibrated compound nucleus.

1.6 Motivation and justification of proposed work:-

1.6.1 Switching of shell gaps:-

New nuclear structure effects concerning the stability of deformed shells are known to be contained in exotic cluster decays [46]. The super deformed *Z*=38, ^{78}Sr nucleus is found to be very stable against all cluster decays whereas the neighboring and equally deformed *Z* = 40, ^{80}Zr is not so stable, at least for some clusters. This result of a very stable deformed shape at *Z(N)* = 38, and not at *Z(N)* = 40, is understood as a switching and new reinforcement shell gap effect of Z=38 deformed shell on N=38 deformed shell. This kind of switching behavior can play a very significant role in the production of super heavy elements, cluster radioactivity and nuclear dynamics related problems.

It is now established that whereas $^{90}_{40}Zr_{50}$ is a doubly magic spherical nucleus is one of the most deformed (called super deformed) nuclei in nature with an estimated quadrupole deformation of β= 0.4[51]. Similarly, in their neighborhood, $^{76}_{38}Sr_{38}$, $^{78}_{38}Sr_{38}$ are super deformed nuclei [52-53] and $^{88}_{38}Sr_{38}$ is a nearly double magic spherical nucleus. This is shown in Figure 1.5, where the quadrupole deformations β, estimated from Grodzin's formula [54], are plotted. Observations of such large ground-state deformations for Z(N) = 38,40 nuclei call for a natural breaking of spherical shell closures at Z = N = 40. This leads to instability of these nuclei against exotic cluster decay modes. The calculations of [55] show that $^{80}_{40}Zr_{50}$, though stable against alpha decay, is metastable (having positive Q values) with respect to many heavier clusters (with $A_2 \geq 16$).

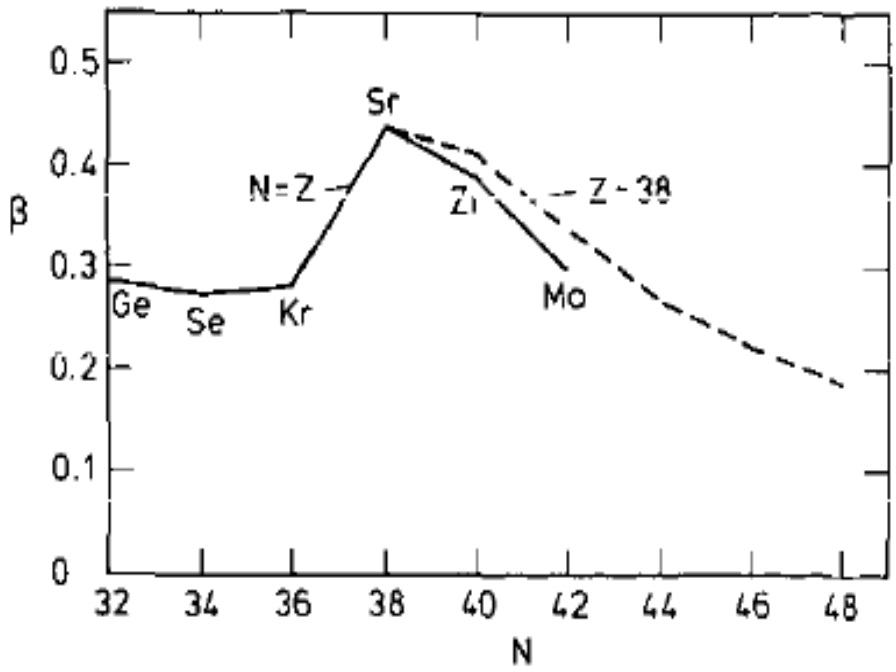

Figure.1.5: The quadrupole deformations β, calculated from Grodzins' formula $\beta_2 = 1225/(A^{7/3} E_{2+})$, plotted as a function of neutron number *N* for *N* = *Z* and *Z* = 38 nuclei.

The calculated half-life times for ^{24}Mg and ^{28}Si decays of ^{80}Zr are of the same order (log $T_{1/2} \approx 43$) as predicted for many cluster decays of heavy deformed 'stable' nuclei [56-58]. In view of this calculation, the neighboring ^{76,78}Sr nuclei with Z = 38, N = 38,40 are expected to be more unstable against exotic cluster decays since they are even more deformed as compared to ^{80}Zr. Also the expected spherical shell closure at Z=40 is already broken in the case of Sr nuclei. It has been observed that the calculated cluster decay half-life times for ^{78}Sr are much larger $(T_{1/2} > 10^{100} s)$ than for its immediate neighboring nucleus ^{80}Zr. Such an unexpected stability of the $^{78}_{38}Sr_{40}$ nucleus against cluster decays must apparently be due to *stable* (deformed) closed shells at Z=N=38, predicted in many earlier calculations [49-50]. The above noted effects of the existence of stable deformed shapes of a doubly magic deformed nucleus at Z=N=38 rather than at Z=N=40 (but Z=40; N = 50 still retaining the double magicity of a

spherical nucleus) can be understood in terms of the reinforcing and switching of shell gaps in nuclei.

It is observed that Z (or N) = 40 is not a spherical magic number until and unless it is reinforced by another spherical magic N (or Z) number. In the absence of such a reinforcement, there is a switch in the importance of Z(or N) =40 spherical to *Z(or N)* = 38 deformed shell. Thus, $^{90}_{40}Zr_{50}$ is a doubly magic spherical nucleus since here the N = 50 spherical magic shell reinforces the Z=40 shell. Similarly, in $^{68}_{28}Ni_{40}$, the *Z=28* spherical magic shell reinforces the *N* = 40 shell to make it a doubly magic spherical nucleus [59]. The same argument applies to the neighbouring spherical nuclei, like $^{88}_{38}Sr_{50}$ and $^{66}_{28}Ni_{38}$ Thus, $^{80}_{40}Zr_{40}$ is apparently an example where the reinforcement effects of a spherical magic number are absent and the switching over to deformed Z(or N) = 38 becomes important. In view of such a switching effect the Z = N = 38, $^{76}_{38}Sr_{38}$ is a doubly magic superdeformed nucleus (see also figure 1.4) and the neighbouring $^{78}_{38}Sr_{40}$ and $^{80}_{40}Zr_{40}$ are strongly deformed nuclei. Here, once again, a new reinforcement shell gap effect of the Z = 38 deformed shell on the N = 38 deformed shell which makes the $^{77,78}Sr$ nuclei far more stable than $^{80}_{40}Zr_{40}$ and other neighbouring nuclei such as $^{72}_{36}Kr_{36}$ and $^{84}_{42}Mo_{42}$ are observed. It is reported in [46] that such strong nuclear structure effects are borne out in the exotic cluster decay studies. In fact, the presence of nuclear shell structure effects in radioactive cluster decays of heavier nuclei is already evident from the observed daughter products, which are always the magic or nearly magic spherical nuclei [60].

It is reported in [45] that ^{76}Sr is a superdeformed nucleus with an estimated quadrupole deformation β_2 = 0.44. From the point of view of known spherical shell closures at *Z*=*N*=40, such a large ground-state deformation for ^{76}Sr means the natural breaking of these spherical shells and hence nuclear instability against both fission and exotic cluster decay processes. However, like the other superdeformed nuclei in this mass region 68-82 although this nucleus is naturally stable (negative *Q* value) against only light clusters with masses A_2<12, the

calculated cluster decay half-lives for A_2>12 are also large enough ($T_{1/2}$>10^{80} s) to term this nucleus as a stable nucleus against all cluster decays. This kind of stability could apparently be due to stable *deformed* shell closures at *Z*=*N*=38, predicted earlier in many other calculations [12,13]. Alternatively, if these nuclei are prepared in heavy-ion collisions, then, depending on the excitation energy of the compound nucleus formed, both fission (also called fusion-fission) and cluster decay are the viable processes. It now seems accepted that compound systems with *A*<42 are characterized by nuclear orbiting phenomenon (the deep inelastic process). Although a considerable amount of yield due to fusion-fission could not be ruled here too [18,19]. On the other hand, the systems with *A*= 47–60 are strongly the cases of fusion-fission processes (fully-energy-damped Fragments) since for all cases studied so far the observed yields are independent of nuclei in the entrance channel and no strong peaking of yields is observed near the target and projectile masses. Thus in [45] calculations for fission and cluster decays of ^{76}Sr, both the cases of ^{76}Sr in the ground state and produced as an excited compound system in heavy ion reactions are studied. where fission is treated as a collective mass transfer process and cluster decay studies are based on a model allowing preformation of clusters. Calculations show that, in a clear asymmetric mass distribution, ^{76}Sr nucleus allows preferential α-nuclei transfer resonances as well as decays.

1.6.2 Relative stability of nuclei in mass region A=68 to 82:-

The mass region A= 68-82 provide a handful of superdeformed nuclei. Obviously, main purpose is to identify the most stable nuclei among all superdeformed fragments in this mass region. The mass region A=68-82 is considered as a small island of superdeformed nuclei, with most of them having quadrupole deformation β_2 = 0.4(or axis ratio 1.5:1), The structural calculations does not indicate that which nucleus lies at the centre of island of superdeformation, because the available data regarding the quadrupole deformation is not sufficient

enough. For example, $_{38}$Sr isotopes with Z=38, 36≤N≤42 are predicted to have β_2 =0.35-0.4. The same work predicts β_2 = 0.38 for $_{36}Kr^{76}$. Even Z=N=40, Zr^{80} is equally deformed with β_2 =0.45. In fact, the same calculation also predicts Z = 36, N = ^{76}Kr nucleus to have a prolate ground state deformation minimum lying at β= 0.38. Furthermore, another weakly prolate deformed (β_2 = 0.22) closed shell is predicted at Z = 34. To answer the question regarding (deformed) magicity among these superdeformed nuclei, a systematic cluster decay study in mass region A=68-82 was carried out by Gupta et.al [44].They exploite the simple idea that a large ground state deformation of nucleus leads to the natural breaking of spherical shell closure making it instable against cluster decays where as the presence of stable deformed closed shell leads to stability against such decay channels.

Thus, it is not clear from these structure calculations, which nucleus lies at the centre of this island of super deformation, i.e. which is most stable. The main aim was to answer this question through a systematic cluster decay study of Z = 34–40 nuclei. A large ground state deformation of a nucleus means the natural breaking of spherical shell closure and hence its possible instability against exotic cluster decays. On the other hand, the presence of a stable, deformed, closed shell for any of its proton or neutron numbers (or both) would lead to its stability against such decay modes.

The basic intension was to explore the relative stability of nuclei with Z = 38, 40 or 50 < Z < 82. Some of the nuclei in this region are found to be unstable against cluster decays [37,38,41] even though they come from the immediate neighborhood of spherical magic numbers. The calculations predicted new magicities in the neighborhood of Z = 74,76, N = 96,100–4, since the daughter products in all the so-far observed cluster decays of actinides[42] are always magic or nearly magic (spherical) nuclei. In this we concentrate on the other region around Z = 38, 40 and extend it to include the total region of superdeformation with A = 68–82 and 34 ≤Z ≤40. It may be noted that the usual competitor, α-decay, is not allowed (Q < 0) in these nuclei, though the

measured[43] β^+-decay half-lives are very small (and hence more probable)—of the magnitude of a few seconds to some minutes, compared with the very high (less probable) half-lives $>10^{10}$ s, predicted for heavy cluster decays.

The Superdeformed $^{78}_{38}Sr_{40}$ is observed to be [36] very stable against exotic cluster decays whereas the neighboring, equally deformed $^{80}_{40}Zr_{40}$ is not so stable. Based on this result, the reinforcing effect of the deformed shell gaps at Z = 38 and N = 38 was expected to give $^{76}_{38}Sr_{38}$ as the most stable superdeformed shape. However, the preliminary analysis of other neighboring nuclei, comprising the mass region A = 68–82, shows that Z = 36, N = 40 ^{76}Kr is the most stable deformed nucleus in this region and as neutrons are added to or subtracted from the most stable isotope (for Sr and Zr nuclei, the most stable isotopes are ^{80}Sr and ^{78}Zr, respectively), the resulting nuclei are highly unstable against all possible (Q > 0) exotic cluster decays. This result of extra stability at Z = 36 and N = 40 is in agreement with the fact that the neighboring Z = 36 ± 2, N = 40 ± 2 nuclei are all deformed and the ones farther away with Z = 36 ± 4, N = 40 ± 4, or more, are (nearly) spherical. Thus, it seems that Z = 36 and N = 40 are better (deformed and/or spherical) closed shells, and the concept of 'switching of shell gaps'. Simply the proximity to shell closures is enough to explain both the deformation and spherical effects of Z = 32–40 nuclei. In the present work we intend to discuss some two-centre shell model calculations in order to resolve this issue of relative stability among various super deformed nuclei. Though the calculations are in preliminary stage, however we find some reasonable statements regarding stability/ instability in this mass region. The other result of strong instability of nuclei in this mass region stresses the role of known spherical magic shells for daughter nuclei in the exotic cluster decay studies [42].

References:

[1] V.M. Strutinsky, Nucl. Phys. A 95, 420 (1967).

[2] W.D Myers and W.J. Swiatecki, Nucl. Phys. 81, 1 (1966).

[3] S.G. Nilsson, J.R. Nix, A. Sobiczewski, Z. Szymanski, S. Wizech, C. Gustafson

and P. M¨oller, Nucl. Phys. A 115, 545 (1968).

[4] S.G. Nilsson, C.F. Tsang, A. Sobiczewski, Z. Szymanski, S. Wycech, C. Gustafson, I.-L. Lamm, P. M¨oller and B. Nilsson, Nucl. Phys. A 131, 1 (1969).

[5] U. Mosel and W. Greiner, Z. Phys. 222, 261 (1969).

[6] E.O. Fizet and J.R. Nix, Nucl. Phys. A 193, 647 (1972).

[7] J. Randrup, S.E. Larsson, P. M¨oller, A. Sobiczewski and A. Lukasiak, Phys. Scr. 10A, 60 (1974).

[8] Z. Patyk and A. Sobiczewski, Nucl. Phys. A 533, 132 (1991).

[9] P. M¨oller and J.R. Nix, Nucl. Phys. A 549, 84 (1992).

[10] P. M¨oller and J.R. Nix, J. Phys. G 20, 1681 (1994).

[11] R. K. Gupta, W. Scheid, and W. Greiner, J. Phys. G **17**, 1731(1991).

[12] P. Mo¨ller and J. R. Nix, Nucl. Phys. **A361**, 117 (1981)

[13] R. Bengtsson, P. Mo¨ller, J. R. Nix Phys. Scr. **29**, 402 (1984).

[14] C. Beck, D. Mahboub, et al. Phys. Rev. C **54**, 227 (1996).

[15] K. A. Farrar, S. J. Sanders,et al. Phys. Rev. C **54**, 1249 (1996).

[16] S. J. Sanders, A. Hasan, et al. Phys. Rev. C **49**, 1016 (1994).

[17] Sl. Cavallaro, C. Beck, Nucl. Phys. **A583**, 161 (1995).

[18] S. J. Sanders, Phys. Rev. C **44**, 2676 (1991).

[19] N. Aissaoui, F. Haas, R. M. Freeman, C. Beck, M. Morsad, B.

[20] S.K. Patra, R.K.Gupta and W. Greiner, Mod. Phys. Lett. A 12, 1727 (1997).

[21] S.K. Patra, R.K.Gupta and W. Greiner, Nucl. Phys. A 651, 117 (1999).

[22] M. Bender et al., Phys. Rev. C 60 034304 (1999).

[23] A.T. Kruppa et al., Phys. Rev. C 61 034313 (2000).

[24] S. Tapaa et al., Phys. Rev. C 69 044315 (2004).
[25] J. Maruhn and W. Greiner, Phys. Rev. Lett. 32, 548 (1974).
[26] R.K. Gupta, W. Scheid and W. Greiner, Phys. Rev. Lett. 35, 353 (1975).
[27] A. Sˇandulescu, R.K. Gupta, W. Scheid and W. Greiner, Phys. Lett. 60B, 225 (1976).
[28] R.K. Gupta, A. Sˇandulescu and W. Greiner, Phys. Lett. 67B, 257 (1977); Rev. Roum. Phys. 23, 51 (1978).
[29] S. Yamaji, W. Scheid, H.J. Fink and W. Greiner, Z. Phys. A 278, 69 (1976).
24
[30] S. Yamaji, W. Scheid, H.J. Fink and W. Greiner, J. Phys. G: Nucl. Phys. 2, L189 (1976).
[31] S. Yamaji, K.H. Ziegenhain, H.J. Fink, W. Greiner and W. Scheid, J. Phys. G: Nucl. Phys. 3, 1283 (1977).
[32] R.K. Gupta, A. Sˇandulescu and W. Greiner, Z. Naturforsch. 32a, 704 (1977).
[33] R.K. Gupta, C. Pirvulescu, A. Sˇandulescu and W. Greiner, Z. Physik A 283, 217 (1977); Sovt. J. Nucl. Phys. 28, 160 (1978).
[34] R.K. Gupta, Z. Physik. A 281, 159 (1977).
[35] A. Sˇandulescu, H.J. Lustig, J. Hahn, and W. Greiner, J. Phys. G: Nucl. Phys.
4, L279 (1978).
[36] Gupta R K, Singh S,W 1991 J.Phys.G:Nucl.Part.Phys.17 1731
[37] [Gupta R K, Singh S, Puri R K and Scheid W 1993 *Phys. Rev.* C **47** 561
[38] Kumar S and Gupta R K 1994 *Phys. Rev.* C **49** 1922
[39] Kumar S, Bir D and Gupta R K 1995 *Phys. Rev.* C **51** 1762
[40] Kumar S, Batra J S and Gupta R K 1996 *J. Phys. G: Nucl. Part. Phys.* **22** 215
[41] Gupta R K 1997 *8th Int. Conf. Nuclear Reaction Mechanisms, June 9–14* (Varenna, Italy)
Gupta R K, Bir D and Dhaulta S 1997 *Mod. Phys. Lett.* A **12** 1775
[42] Gupta R K and Greiner W 1994 *Int. J. Mod. Phys.* E **3** 335

[43] Pfennig G, Klewe-Nebenius H and Seelmann-Eggebert W 1995 *Karlsrule Chart of the Nuclides*

[44] Stability and instability of nuclei in the mass region *A* = 68–82
based on exotic cluster decay studies J. Phys. G: Nucl. Part. Phys. 25 (1999) 1089–1097.

[45] Fission and cluster decay of the ^{76}Sr nucleus in the ground state
and formed in heavy-ion reactions. Raj K. Gupta, Manoj K. Sharma et al.

[46] Raj K Gupta, Werner Scheid and Walter Greiner. J. Phys. G Nucl. Part. Phys. 17 (1991) 1731-1737.

.[47].Hamilton J H, Ramayya A Vet al 1984 J. Phys. G: Nucl. Phys.10 L87

[48] Hamilton I H, Hansen P G and Zganjar E F 1985 Rep. *Prog. Phys.* 48 631

[49] Moller P and Nix J R 1981 Nucl. *Phys.* A 361 117; 1981 At. *Dala* Nucl. Data *Tables* 26 165

[50] Bengtsson R, Moller P, Nix J R and Zhang J-Y 1984 *Phys. Scr.* 29 402

[51] Lister C J, Campbell et al 1987 *Phys. Rev. Len. 59* 1270

[52] Gross C et al 1989 *Phys. Rev.* C 39 1780

[53] Lister C J, James A N 1988 *Int. Workrhop on Nuclear Strucrure of (he Zirconium Region*(Berlin: Springer) p 298

[54] Grnizins L 1962 Phys. *Len.* 2 *88;* et al. 1972 *Phys. Reu. Lerl. 29* 438

[55] Puri R K, Malik *S* S and Gupta R K 1989 *Europhys. Lett 9* 767

[56] Malik S S, Singh , Gupta R K 1989 *Promono 1. Phys. 32* 419, 989 *Proc. 50*

[57] Poenaru D N, Greiner W, Ivascu M and Sandulescu A 1985 *Phys. Rev.* C *32* 2198

[58] Poenaru D N, Greiner W, Depta K, Ivascu M, Mazilu 0 and Sandulescu A 1986 *Al. Dora* Nucl.

[59] Bemas M, Dessagne Ph, Langevin M, Payet J, Pougheon F and Roussel P 1982 *Phys. Leu.* 1UB 279

[60] Price P B 1989 *Ann. Reu. Nucl. Pad.* Sci. *39* 19

Chapter 2

METHODOLOGY

2.1 **Introduction**:-

Nuclear dynamics and structure related problems can be addressed successfully using dynamical cluster decay model (DCM) which is based on the well established quantum mechanical fragmentation theory (QMFT). The main advantage of DCM over other statistical models is that it treats the light particles (LP's) and Intermediate mass fragments (IMF's) on equal footings, whereas in all other statistical models the LP's and IMF's are treated differently. Another important feature of DCM is that it involves the preformation probability P_0 of the decaying fragments and hence imparts the important structure information. In the present work, the single particle energies are calculated using the Two-center shell model (TCSM). The two center shell model predicts successfully the information regarding single-particle inelastic excitations neutron transfer reactions along with various nuclear structures and dynamics related problems.

2.2 Two Center Shell Model:-

The theoretical study of binary disintegration processes is limited by the difficulties encountered in the calculations of single-particle levels for very deformed one-center potentials. Indeed, on one hand, central potentials are not able to describe in a correct manner the shapes for the passage of one nucleus to two separated nuclei and, on other hand, for very large prolate deformations the sum of single-particle energies obtained from the level scheme reaches an infinite value. These difficulties are surpassed by considering that the mean field is generated by nucleons moving in a double center potential. A two-center model allows the description of single-particle energy evolutions from the ground-state up to the formation of two separated fragments [1, 2] of a dinuclear system. Most of the applications of this method are based on a double oscillator potential [3] and more recently, the single-particle motion in fusioning systems and the

peripheral collisions were treated employing Wood-Saxon wells [4] with the potential expansion method. A new version of the two-center model, namely the super asymmetric two center shell model (STCSM) was developed [5–7] and was used to explain the fine structure in alpha- and cluster decays [6, 8].

The renewal interest for the fission physics determined the use of the STCSM in the analysis of the role played by the single-particle states during the tunneling of the double barrier. Information about the role of the dissipation and effects due to the dynamics were revealed [9–11]. Investigating fission processes, unfortunately, very large values of the heights of the double barrier were obtained. A cause for this behavior was presumed to be due to the intrinsic limitations of the modified oscillator model [7]. The angular momentum interaction constants are determined only to fit several single particle levels in the vicinity of the Fermi energy and are not appropriate for all the levels taken into account when the shell effects are computed. On the other hand, the spin-orbit operator cannot take into account a realistic deformed mean field potential. In the following, a improved version of a two center shell model is presented that takes into account Woods-Saxon potentials.

In principle, a two-center diagram can be used to investigate all reactions that involve two separated nuclei. On one hand, it is possible to predict which single-particle inelastic excitations and neutron transfer reaction will be enhanced in heavy ion collisions. On another hand, it is also possible to determine the transition levels for the fission reactions, leading to a improved calculation of the fission cross-sections. It is customary for evaluation purpose to fit the transition levels from experimental values of the cross-sections.

A realistic model for the single-particle energies able to describe the passage from one nucleus in two separated fragments will provide a powerful tool to validate the evaluations. A realistic model for the level scheme can also provide information about important quantities as the dissipation by solving the microscopic equations of motion.

The two-centre shell model, used within the Strutinsky macro–microscopic method, is a valid prescription for calculating adiabatic or diabatic potential

energy surfaces. It is shown, however, that this model does not contain the appropriate α-nucleus structure effects, very much required for collisions between light nuclei. The TCSM has also been used quite extensively for calculating the PES, both for the light and heavy nuclei.

The importance of shell effects is a result of inability of liquid drop model alone to give a satisfactory description of both fission and heavy ion collision phenomena. The natural starting point is the simple one centre shell model (Nilson oscillator potential or finite depth Woods-Saxon potential). However, for nuclear shapes involving large deformations and neck formation, it is intuitively more realistic to use two centers of force. An asymmetric two centre shell model (ATCSM) was developed by Maruhn and Greiner. Such a potential and associated nuclear shapes (for protons and neutrons moving in two separate single particle oscillator are shown in Figure 2.1

The following naturally occurring parameters are used to characterize the shape:
(1) The relative separation R of the two fragments, or the elongation λ =($2R_0$), which measures the length "L" of the system in units of the diameter ($2R_0$) of the equivalent spherical compound nucleus.
(2) The deformations of the two fragments, which for the rotational symmetry around the z-axis are defined by $\beta_i = \frac{a_i}{b_i}$, i = 1, 2, the ratio of their semi-axes.

(3) The neck parameter " $\varepsilon = \frac{E_0}{E}$ ", defined by the ratio of the actual barrier height E_0 to the fixed barrier height E' of the two-centre oscillator, given by

$$E = \frac{1}{2} m_0 \omega^2 Z_0^2 = \frac{1}{2} m_0 \omega_{Z_1}^2 Z_1^2 = \frac{1}{2} m_0 \omega_{Z_2}^2 Z_2^2$$

This relation ensures that the barrier must have the same position on Z-axis as in the two center oscillator.

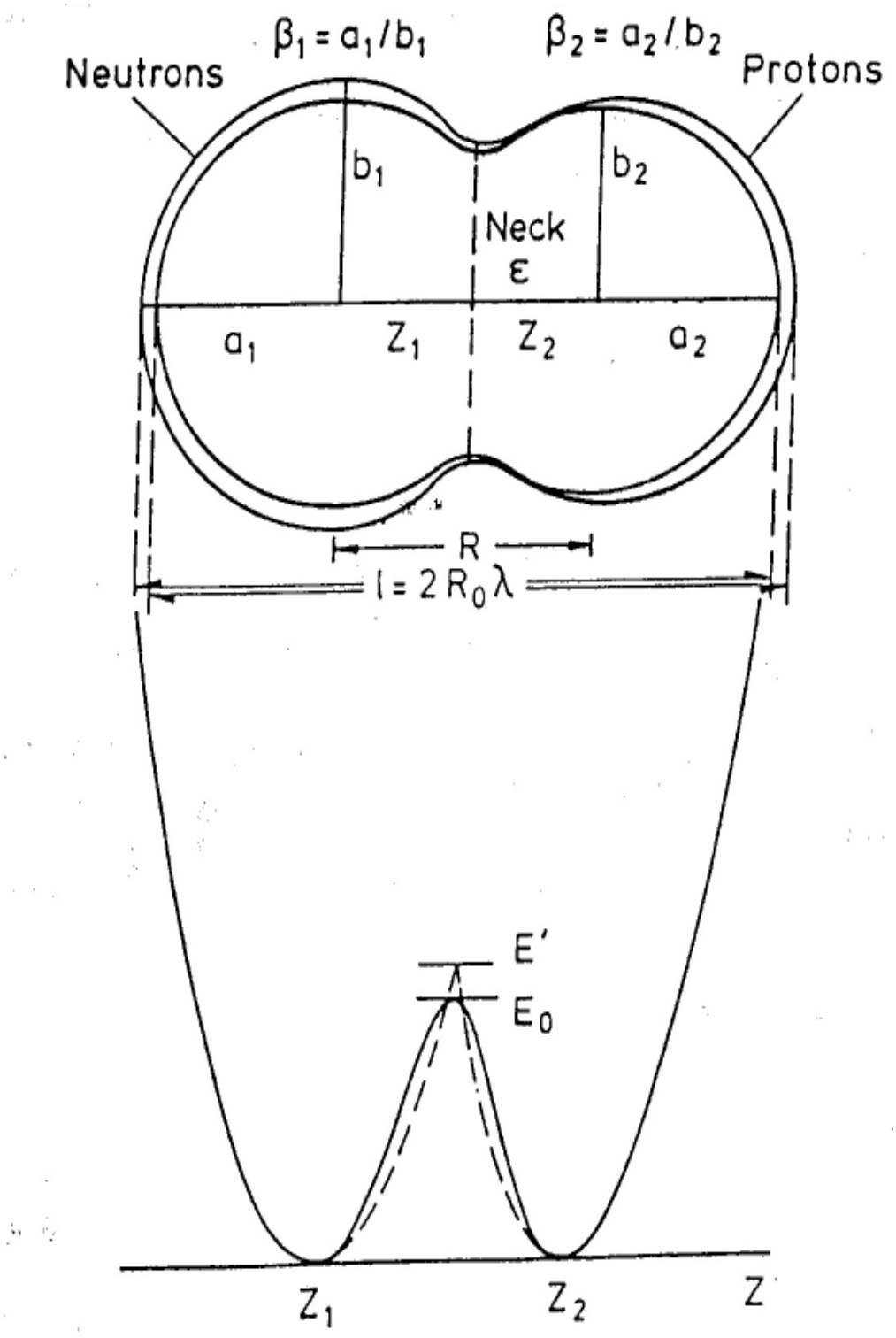

Figure.2.1: Asymmetric two centre shell model (ATCSM) potential and the associated nuclear shapes for protons and neutrons.

(4) The mass and charge asymmetry coordinates

$$Q = \frac{\omega_{\rho 2}}{\omega_{\rho 1}} = \frac{\beta_2 \omega_{Z_2}}{\beta_1 \omega_{Z_1}}$$

This is not immediately related to the mass ratio of the fragments, except for zero separation and for separated fragments where one has purely ellipsoidal fragments with a mass (volume) ratio

$$\frac{V_1}{V_2} = \frac{a_1 b_1^2}{a_2 b_2^2} = \frac{\beta_1}{\beta_2} Q^3$$

In this limit Q is directly related to the basic mass fragmentation coordinate of the dynamical fragmentation theory.

The potential of the ATCSM is (i=1,2)

$$V(\rho, Z) = \begin{cases} \frac{1}{2} m_0 \omega_{Z_1}^2 (Z'^2 + \beta_1^2 \rho^2) Z < Z_1 \\ \frac{1}{2} m_0 \omega_{Z_1}^2 (Z'^2 f_0 (1 + c_i Z' + d_i Z'^2) + \frac{1}{2} m_0 \omega_{Z_i} \beta_i \rho^2 (1 + g_i Z'^2) Z_1 < Z < Z_2 \\ \frac{1}{2} m_0 \omega_{Z_2}^2 (Z'^2 + \beta_2^2 \rho^2) Z > Z_2 \end{cases}$$

where

$$Z' = \begin{cases} Z - Z_1, Z < 0 \\ Z - Z_2, Z > 0 \end{cases}$$

2.2.1 <u>Strutinsky macro-microscopic method:-</u>

Strutinsky gave a method to extract the shell correction to liquid drop model (LDM) energy from the shell model itself. According to this, so called, macro-microscopic method, the smooth part of the binding energy is given by LDM (the macroscopic part) and the small fluctuations, of the order of 5-10 MeV due to shape of the nucleus, must be associated with the shell structure of nucleus (microscopic part) and hence contained in shell model single particle energies at

a given deformation β of average potential. Thus, the macroscopic LDM energy and the microscopic shell correction were put together to give the binding energy of the nucleus as

$$V(\beta) = V(LDM) + \sum_{n,p} (\delta U + \delta P),$$

where

$$\delta U = \sum_{i=1}^{F} [\varepsilon(\beta) - \bar{\varepsilon}(\beta)],$$

with $\bar{\varepsilon}(\beta)$ defining the uniform single particle energies. δP is the pairing correction energy.

2.3Quantum Mechanical Fragmentation Theory (QMFT):-

Cluster radioactivity, cold fission and cold fusion of nuclei for synthesizing new heavy elements are rare nuclear processes. The interesting aspect of these processes is that they are not only rare but also occur more probable as cold phenomena. The rare nature of these processes stem from the fact that these processes are masked by other competing processes. Cluster radioactivity is masked by the larger number of α-decay events, cold fission by fragments of various other velocities (hot and/or bimodal fission) and cold fusion by their specific choice of target-projectile combinations, incident bombarding energies and angular momenta. The dynamical or quantum mechanical fragmentation theory (QMFT) predicted all the three phenomena to be most probable as cold processes. These predictions were made as early as in 1974–75, *prior* to their being observed experimentally. Note that the QMFT, being a quantum mechanical theory, does not preclude the other processes, like the hot fission or hot fusion, but predict them to be less probable, as is now observed to be the case.

Cluster radioactivity is the spontaneous emission of clusters heavier than α particle and *without* being accompanied by any neutron emission. Thus, it is a cold process (zero excitation energy) since the energy released as Q-value is completely consumed by the kinetic energy alone of the two fragments (the

cluster and daughter nuclei). Fission is also the spontaneous breaking of a nucleus into two fragments (for binary fission), heavier than the ones involved in cluster radioactivity, but with or without being accompanied by neutron emission. The neutron less fission or in terms of velocities the very high *total kinetic energy* (Close to the Q-value) fission, called cold fission, The QMFT is a unified description of all the three processes of (cold) fusion, fission and cluster radioactivity. The key result behind the three phenomena is the shell closure effect of one or both of the reaction partners for fusion or that of the decay products for fission and cluster radioactivity. Both experimentally and theoretically, for cold phenomena, one of the nucleus (or decay product) is always a *spherical* closed or nearly closed shell nucleus. Apparently, the significance of spherical closed shells raises the question of the role of *deformed* closed shells, which need to be investigated. The QMFT is applied very successfully to many heavy ion reactions, the predictions of target-projectile combinations for cold synthesis of new and superheavy elements, the fission data and the exotic cluster decay process. In fact, both the phenomena of cold fission and cluster radioactivity were predicted on the basis of this theory, *prior* to their experimental observations, and the idea of cold fusion (for synthesis of new elements) was first introduced on the basis of this theory.

2.4 The Preformed Cluster-decay Model for ground state decay of nucleus:-

These models fall into two main categories:

i) Unified Fission models (UFM), and

ii) Preformed cluster-decay models (PCM).

In the *UFM*, the cluster decay is dealt simply as a barrier penetration problem where as the preformed cluster model (PCM) distinguishes itself from the unified fission model (UFM) in its basic assumption of the emitted cluster(s) being preborn in the parent nucleus with a probability that decreases with the increasing size of the cluster. This suggests that the process of cluster decay will

stop somewhere and that of fission will take over, with a possible overlap for some region. It is seen that such an overlap does exist indeed for clusters of masses $42 < A_2 < 50$.

The PCM is developed as a further modification of the Gamow theory, considering not only the penetration of a realistic barrier (coulomb + nuclear, as in UFM), but also associating a preformation probability P_0 to the emitting cluster. Thus, the decay constant in the PCM is defined by

$$\lambda^{PCM} = \upsilon_0 P P_0 \qquad \text{--- (2.1)}$$

Here υ_0 is the impinging frequency with which the cluster hits the barrier, given by

$$\upsilon_0 = \upsilon/R_0 = \frac{(2E_2/\mu)^{1/2}}{R_0} \qquad \text{--- (2.2)}$$

where R_0 is the radius of parent nucleus and $E_2 = \frac{1}{2}\,\mu\, v^2$ is the kinetic energy of the emitted cluster. The impinging frequency υ_0 is nearly constant~ 10^{21} s^{-1} for all the observed cluster decays. since both the emitted cluster and daughter nuclei are produced in ground state, the entire positive Q-value of decay is the total kinetic energy, ($Q = E_1 + E_2$), available for the decay process, which is shared between the two fragments, such that for the emitted cluster,

$$E_2 = \frac{A_1}{A} Q \qquad \text{--- (2.3)}$$

and, E_1 ($=Q - E_2$) is the recoil energy of daughter nucleus. P_0 is preformation probability of the cluster, and P is the WKB penetration probability of cluster through the barrier, calculated within the QMFT.

The QMFT is worked out in terms of the collective coordinates of mass and charge asymmetries

$$\eta = \frac{A_1 - A_2}{A_1 + A_2} \qquad \text{and} \qquad \eta_z = \frac{Z_1 - Z_2}{Z_1 + Z_2},$$

(1 and 2 stand, respectively, for daughter and cluster) and the relative separation R, to which are added the multipole deformations $\beta_{\lambda i}$ and orientations θ_i (i=1,2) of daughter and cluster nuclei. In PCM, the two coordinates η and R refer, respectively, to the nucleon-division (or-exchange) between the daughter and cluster, and the transfer of positive Q-value to the total kinetic energy ($E_1 + E_2$) of two nuclei as they are produced in the ground state, as already pointed out above.

The preformation probability $P_0(A_i)$ ($\equiv |\Psi(\eta(A_i))|^2$, i=1 or 2) is the solution of the stationary Schrodinger equation in η, at fixed $R = R_a$, the first turning point of the penetration path used for calculating the penetrability P. Thus, the structure information of the compound nucleus is contained in P_0 via the fragmentation potential

$$V_R(\eta) = -\sum_{i=1}^{2}[Bi(Ai, Zi)] + V_c(R, Z_i, \beta_{\lambda i}, \theta_i) + V_p(R, A_i, \beta_{\lambda i}, \theta_i) + V_l(R, A_i, \beta_{\lambda i}, \theta_i) \quad \text{--(2.4)}$$

used in the above said stationary Schrödinger equation. Here, $B_i(A_i, Z_i)$ are the ground state binding energies from Ref. [12], and V_c, V_p, and V_l are, respectively, the Coulomb, nuclear proximity, and angular- momentum dependant potentials. For ground-state decays, l=0 is a good approximation [4].

In Eq. (4), the proximity potential V_p for deformed and oriented nuclei is given as,

$$V_P(s_0) = 4\pi\bar{R}\gamma b\,\phi(s_0) \quad \text{--- (2.5)}$$

With the specific nuclear surface tension coefficient γ = 0.9517 [1- 1.7826 $\left(\frac{N-Z}{A}\right)^2$] MeV fm^{-2}, the surface thickness b =0.99 fm, and the universal, function, independent of the geometry of nuclear system, is

$$\phi(s_0) = \begin{cases} -\frac{1}{2}(s_0 - 2.54)^2 - 0.0852(s_0 - 2.54)^3 \\ -3.437\exp(-s_0/0.75) \end{cases} \quad \text{--- (2.6)}$$

respectively, for $s_0 \leq 1.2511$ and ≥ 1.2511. Here, s_0 is in units of surface thickness b. For determining the shortest distance s_0 between any two colliding

nuclei, we use the expression of Gupta et al. [13], obtained for all possible orientations of two equal or unequal, axially symmetric, deformed nuclei lying in one plane,

$$s_0=R-X_1-X_2 \quad \text{--- (2.7)}$$

where $X_1=R_1(\alpha_1)\cos(\theta_1-\alpha_1)$ and --- (2.8)

$$X_2=R_2(\alpha_2)\cos(180+\theta_2-\alpha_2) \quad \text{--- (2.9)}$$

are the projections along the collision Z –axis of nuclei. The mean curvature radius R' in Eq. (2.5) for two co-planar nuclei is

$$\frac{1}{\overline{R}^2}=\frac{1}{R_{11}R_{12}}+\frac{1}{R_{21}R_{22}}+\frac{1}{R_{11}R_{22}}+\frac{1}{R_{21}R_{12}} \quad \text{--- (2.10)}$$

with the four principal radii of curvature R_{i1} and R_{i2} of the two reaction partners given by Eq. (4) of [13], and the radius vectors

$$R_i(\alpha_i)=R_{0i}\left[1+\sum_{\lambda}\beta_{\lambda i}Y_{\lambda}^{(0)}(\alpha_i)\right] \quad \text{--- (2.11)}$$

with the R_{0i} given by

$$R_{0i}=1.28A_i^{1/3}-0.76+0.8A_i^{-1/3} \quad \text{--- (2.12)}$$

For Coulomb interaction, extended is [14] expression for two non-overlapping charge distributions, to all higher multipole deformations (λ=2, 3, 4..), is [36]

$$V_C=\frac{Z_1Z_2e^2}{R}+3Z_1Z_2e^2\sum_{\lambda,i=1,2}\frac{1}{2\lambda+1}\frac{R_i^{\lambda}(\alpha_i)}{R^{\lambda+1}}Y_{\lambda}^{(0)}(\theta_i)\left[\beta_{\lambda i}+\frac{4}{7}\beta_{\lambda i}^2Y_{\lambda}^{(0)}(\theta_i)\right], \quad \text{--- (2.13)}$$

The mass parameters $B_{\eta\eta}(\eta)$, entering the P_0 calculation via the kinetic energy term, are the smooth classical hydrodynamical masses [15], used for reasons of simplicity. The penetrability P is the WKB integral between R_a and R_b, the first and second turning points, respectively (Fig.2.2). In other words, the tunneling

begins at R= R_a and terminates at R=R_b, with V(R_b) = Q-value for ground state decay. Thus, as per Fig.2.2, the transmission probability P consists of the following three contributions

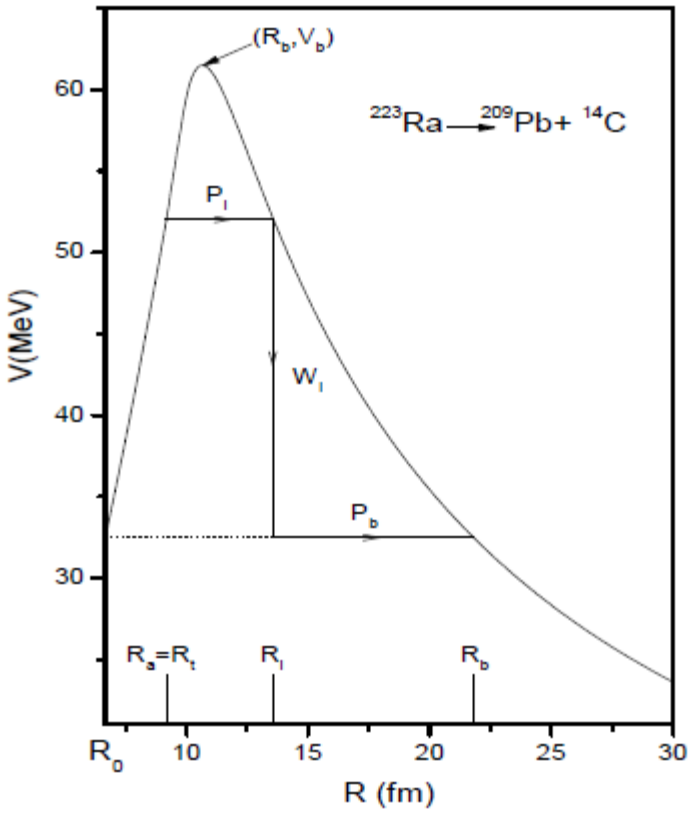

Figure.2.2:: A typical scattering potential, with characteristic quantities marked in it.

1. The penetrability P_i from R_a to R_i,
2. The (inner) de-excitation probability W_i at R_i, and
3. The penetrability P_b from R_i to R_b.

giving the penetration probability as

$$P=P_iW_iP_b \qquad \text{--- (2.14)}$$

The shifting of first turning point from R_a to R_0, the compound nucleus radius, gives the penetrability P similar to that of Shi and Swiatecki [16] for spherical nuclei, which is known not to fit the experimental data without the adjustment of assault frequency. Following the excitation model of M.Greiner and W. Scheid [41] , we take the de-excitation probability W_i=1 for a heavy cluster decays, which reduces Eq.(2.14) to the following:

$$P=P_iP_b\ , \qquad \text{--- (2.15)}$$

Where P_i and P_b in WKB approximation are

$$P_i = \exp[-\frac{2}{\hbar}\int_{R_a}^{R_{ii}}\{2\mu[V(R)-V(R_i)]\}^{1/2}dR] \qquad \text{--- (2.16)}$$

and

$$P_b = \exp[-\frac{2}{\hbar}\int_{R_i}^{R_b}\{2\mu[V(R)-Q]\}^{1/2}dR] \qquad \text{--- (2.17)}$$

For the first turning point, we use the following postulate

$$R_a(\eta) = R_1(\alpha_1) + R_2(\alpha_2) + \Delta R$$

$$= R_t(\alpha,\eta) + \Delta R$$

Where the η- dependence of R_a is contained in R_t, and ΔR is a parameter, assimilating the neck formation effects of two centre shell model [1-11].

Dynamical Cluster-decay Model:

The dynamical cluster-decay model [17] is an adaptation of the preformed cluster model (PCM) of Gupta et al. [18,19] for ground state decays, which itself is based on the well-known Quantum Mechanical Fragmentation Theory, the QMFT [20-22], given for fission and heavy ion reactions. This theory is worked out in terms of the collective coordinates of mass asymmetry $\eta = (A_1 - A_2)/(A_1 + A_2)$ and

relative separation R, which in a PCM allows defining the decay half-life $T_{1/2}$, or the decay constant λ, as

$$\lambda = \frac{\ln 2}{T_{1/2}} = P_0 \nu_0 P \qquad \text{--- (2.18)}$$

where the preformation probability P_0 refers to η motion and the penetrability P to R motion. Apparently, the two motions are taken as decoupled, an assumption justified in the earlier works [20, 21, 23]. The ν_0 is the barrier assault frequency. In terms of the partial waves, the decay cross-section

$$\sigma = \frac{\pi}{k^2} \sum_{l=0}^{l_c} (2l+1) P_0 P \ ; \qquad k = \sqrt{\frac{2\mu E_{c.m}}{\hbar^2}} \qquad \text{--- (2.19)}$$

with $\mu = [A_1 A_2 / (A_1 + A_2)]m = \frac{1}{4} Am(1-\eta^2)$ the reduced mass, l_c (the critical angular momentum), and m is the nucleon mass. This means that λ in Eq. (2.18) gives the s-wave cross-section, with a normalization constant ν_0, instead of the π / k^2 in Eq. (2.19).

For η-motion, we solve the stationary Schrödinger equation in η, at a fixed R,

$$\left\{ -\frac{\hbar^2}{2\sqrt{B_{\eta\eta}}} \frac{\partial}{\partial \eta} \frac{1}{\sqrt{B_{\eta\eta}}} \frac{\partial}{\partial \eta} + V_R(\eta, T) \right\} \psi^{\nu}(\eta) = E^{\nu} \psi^{\nu}(\eta) \text{ -- (2.20)}$$

with ν =0,1,2,3,…..and $R = R_a = C_t (= C_1 + C_2)$, the first turning point, fixed empirically for the ground state $(T = 0)$ decay. This value of R (instead of the compound nucleus radius R_0) assimilates to a good extent the effects of both deformations β_i of two fragments and neck formation between them [24]. The deformation effects of nuclei in the calculations are further included via the Suessmann central radii $C_t = R_i - (b^2 / R_i)$, with radii $R_i = 1.28 A_i^{1/3} - 0.76 + 0.8 A_i^{-1/3}$ fm and the surface thickness parameter $b = 0.99$ fm.

The eigensolutions of Eq. (20) give the preformation probability

$$P_0 = \sqrt{B_{\eta\eta}} \left| \psi[\eta(A_i)] \right|^2 (2/A), \qquad \text{--- (2.21)}$$

(i=1 or 2), where $\psi(\eta)$ is $\psi^{\nu=0}(\eta)$ if the ground-state solution is chosen.

However, for the decay of a hot compound nucleus, we use an ansatz [25] for the first turning point,

$$R_a = C_t(\eta,T) + \Delta R(\eta,T), \qquad \text{--- (2.22)}$$

which depends on the total kinetic energy TKE(T). The corresponding potential $V(R_a)$ acts like an effective, positive Q value, Q_{eff}, for the decay of the hot compound nucleus at temperature T to two fragments in the exit channel observed in the ground states $(T=0)$. Thus, in terms of the respective binding energies B, Q_{eff} is defined as

$$\begin{aligned} Q_{eff}(T) &= B(T) - [B_1(T=0) + B_2(T=0)] \\ &= TKE(T) = V(R_a) \end{aligned} \qquad \text{--- (2.23)}$$

Since, $R_a = C_t(\eta)$ for $T=0$, $\Delta R(\eta)$ corresponds to the change in TKE at T with respect to its value at $T=0$, and hence can be estimated exactly for the temperature effects in the scattering potential $V(R)$.

At temperature T, the preformation factor P_0 in Eq. (2.21) is calculated at $R_a = C_t(\eta) + \overline{\Delta R}$, with the temperature effects also included in $\psi(\eta)$ through a Boltzmann-like function,

$$|\psi|^2 = \sum_{\nu=0}^{\infty} |\psi^{\nu}|^2 \exp(-E^{\nu}/T), \qquad \text{--- (2.24)}$$

with the compound nucleus temperature T (in MeV) related as

$$E^*_{CN} = \left(\frac{A}{9}\right)T^2 - T\,; \qquad \text{--- (2.25)}$$

and for the penetrability P, Eqs. (2.23) for each η and T values mean that

$$V(R_a) = V(C_t + \overline{\Delta R}) = V(R_b) = Q_{eff}(\overline{\Delta R}) = TKE(T) \qquad \text{--- (2.26)}$$

with R_b as the second turning point. The penetrability P is calculated as the WKB tunneling probability, solved analytically in Ref. [21,22].

$$P = \exp\left[-\frac{2}{\hbar}\int_{R_a}^{R_b}\{2\mu[V(R) - Q_{eff}]\}^{1/2}\,dR\right] \qquad \text{--- (2.27)}$$

The fragmentation potential $V_R(\eta,T)$ at any temperature T, is calculated within the Strutinsky renormalization procedure, as

$$V_R(\eta,T) = \sum_{i=1}^{2}[V_{LDM}(A_i,Z_i,T)] + \sum_{i=1}^{2}[\delta U_i]\exp(-T^2/T_0^2) + E_c(T) + V_P(T) + V_l(T) \quad (2.28)$$

where the T-dependent liquid drop energy $V_{LDM}(T)$ is that of Ref. [26], with (Seeger's) constant at $T=0$ refitted to give binding energies of [27]' defined as $B = V_{LDM}(T=0) + \delta U$. The shell corrections are calculated in the "empirical method'' of Myers and Swiatecki [28].

The V_P is an additional attraction due to the nuclear proximity potential [32]' which is also considered temperature dependent here,

$$V_P(R,T) = 4\pi\bar{R}(T)\gamma b(T)\phi(s,T), \quad \text{--- (2.29)}$$

where $\bar{R}(T)$ and $\phi(s,T)$ are, respectively, the inverse of the root mean square radius of the Gaussian curvature and the universal function, which is independent of the geometry of the system, given by Equation. 2.6

$$\bar{R}(T) = \frac{C_1(T)C_2(T)}{C_t(T)} \quad \text{--- (2.30)}$$

and γ is the specific nuclear surface tension given by

$$\gamma = 0.9517\left[1 - 1.7826\left(\frac{N-Z}{A}\right)^2\right]\text{MeV fm}^{-2} \quad \text{--- (2.31)}$$

In Eq. (2.29), $s(T)(=[R-C_t(T)]/b(T)$ is the overlap distance, in units of b, between the colliding surfaces. The temperature dependence in radii R_i is given as [26, 30]

$$R_i(T) = r_0(T)A_i^{1/3} = 1.07(1+0.01T)A_i^{1/3} \quad \text{--- (2.32)}$$

with the surface width

$$b(T) = 0.99(1-0.99T^2) \quad \text{--- (2.33)}$$

The same temperature dependence of $R(T)$ is also used for Coulomb potential $E_c(T) = Z_1Z_2e^2/R(T)$, where the charges Z_i are fixed by minimizing the

potential $V_R(\eta,T)$ in the charge asymmetry coordinate.The shell corrections δU in the Eq. (2.28) are considered to vanish exponentially for $T_0 = 1.5$ Mev [31].

Also, for the angular momentum effects

$$V_l(T) = \frac{\hbar^2 l(l+1)}{2I(T)}. \qquad \text{--- (2.34)}$$

In the non sticking limit, where $R_a = C_1(T) + C_2(T) + \Delta R = C_t(T) + \Delta R$, the moment of inertia in Eq. (2.34) is given by

$$I(T) = I_{NS}(T) = \mu R_a^2. \qquad \text{--- (2.35)}$$

In this case, the separation distance ΔR is assumed to be beyond the range of nuclear proximity forces, which is about 2 fm. However, when it is within the range of nuclear proximity (<2 fm), we get in the complete sticking limit

$$I(T) = I_s(T) = \mu R_a^2 + \frac{2}{5} A_1 m C_1^2 + \frac{2}{5} A_2 m C_2^2. \qquad \text{--- (2.36)}$$

For the l value, in terms of the bombarding energy $E_{c.m.}$ of the entrance channel η_{in} , we have

$$l = l_c = R_a \sqrt{2\mu[E_{c.m.} - V(R_a, \eta_{in}, l=0)]}/\hbar. \qquad \text{--- (2.37)}$$

The mass parameters $B_{\eta\eta}(\eta)$, representing the kinetic energy part in Eq. (2.20), are the smooth classical hydrodynamical masses [35], since at high temperatures the shell effects are almost completely washed out.

Finally, the temperature-dependent scattering potential $V(R,T)$, normalized to exit channel binding energy, is

$$V(R,T) = Z_1 Z_2 e^2 / R(T) + V_P(T) + V_l(T) \qquad \text{--- (2.38)}$$

This means that all the energies are measured with respect to $B_1(T) + B_2(T)$, and the fragments go to ground state $(T \to 0)$ via the emission of light particle(s) and/or $\gamma-$rays of energy E_x.

Oriented Collisions:

For the deformation and orientation effects we use the model developed at Chandigarh by Gupta and collaborators [3]. The potential V for orientated nuclei is the sum of two binding energies B_i and deformation and orientation dependent Coulomb and proximity potentials:

$$V(\eta, R) = -\sum_{i=1}^{2} B_i(A_i, Z_i, \beta_{\lambda i}) + E_C(Z_i, \beta_{\lambda i}, \theta_i) + V_P(A_i, \beta_{\lambda i}, \theta_i) \quad \text{--- (2.40)}$$

The Coulomb and proximity potentials with higher multipole deformations included, are obtained respectively as:

$$E_C = \frac{Z_1 Z_2 e^2}{R} + 3Z_1 Z_2 e^2 \sum_{\lambda, i=1,2} \frac{1}{2\lambda+1} \frac{R_{0i}^{\lambda}}{R^{\lambda+1}} Y_{\lambda}^{(0)}(\alpha_i) \left[\beta_{\lambda i} + \frac{4}{7} \beta_{\lambda i}^2 Y_{\lambda}^{(0)}(\alpha_i) \delta_{\lambda,2} \right] \quad (2.41)$$

with $R_i(\alpha_i) = R_{0i}\left[1 + \sum_{\lambda} \beta_{\lambda i} Y_{\lambda}^{(0)}(\alpha_i)\right]$ and $R_{0i} = 1.28A_i^{1/3} - 0.78 + 0.8A_i^{-1/3}$

The nuclear proximity potential is given as,

$$V_P = 4\pi \bar{R} \gamma b \phi(s_0) \quad \text{--- (2.42)}$$

where the surface energy coefficient $\gamma = 0.9517\left[1 - 1.78269(N-Z)^2 / A^2\right]$ Mev fm^{-1} ; the surface thickness $b \approx 1$fm; $\bar{R}$ is the mean curvature radius given as; $\frac{1}{\bar{R}^2} = \frac{1}{R_{11}R_{12}} + \frac{1}{R_{21}R_{22}} + \frac{1}{R_{11}R_{22}} + \frac{1}{R_{21}R_{12}}$ where the four principal radii of curvature R_{i1} and R_{i2} at the points D and E of minimum s_0, and the universal function, independent or the geometry of nuclear system is given in Equation 2.6

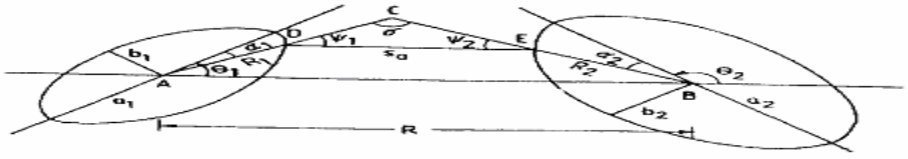

Figure. 2.3: Schematic configurations of two axially symmetric deformed, oriented nuclei.

References:

1. P. Holzer, U. Mosel and W. Greiner, Nucl. Phys., A 138, 241 (1969).

2. J. Maruhn and W. Greiner, Z. Phys., 251, 431 (1972).

3. W. Greiner, J.Y. Park andW. Scheid, in *Nuclear Molecules*, World Scientific, Singapore,
1994.

4. A. Diaz-Torres and W. Scheid, Nucl. Phys., A 757, 373 (2005).

5. M. Mirea, Phys. Rev., C 54, 302 (1996).

6. M. Mirea, Phys. Rev., C 57, 2484 (1998).

7. M. Mirea, Nucl. Phys., A 780, 13 (2006)

8. M. Mirea, Phys. Rev., C 63, 034603 (2001).

9. M. Mirea, L. Tassan-Got, C. Stephan, C.O. Bacri and R.C. Bobulescu, Europhys. Lett.,73, 705 (2006).

10. M. Mirea, L. Tassan-Got, C. Stephan, C.O. Bacri, P. Stoica and R.C. Bobulescu, J.Phys., G 31, 1165 (2005).

11. M. Mirea, L. Tassan-Got, C. Stephan and C.O. Bacri, Nucl. Phys., A 735, 21 (2004).

12. P.Moller, J.R. Nix, W.D. Myers, and W.J. Swiatecki, At. Data Nucl. Data Tables 59, 185 (1995)

13. R.K. Gupta, N.Singh, and M.Mahhas, Phys.Rev. 70, 034608 (2004)

14. C.Y. Wong, Phy.Rev.Lett.31, 766 (1973)

15. H. Kroger and W. Scheid, J. Phys. G 6, L85 (1980)

16. Y.J. Shi and W.J. Swiatecki, Phys.Rev. C 54, 300 (1985)

17. R.K. Gupta, R. Kumar, N.K. Dhiman, M. Balasubramaniam, W. Scheid, and C. Beck, Phys. Rev. C 68, 014610 (2003); M. Balasubramaniam, R. Kumar, R.K. Gupta, C. Beck, and W. Scheid, J. Phy. G: Nucl. Part. Phys. 29, 2703 (2003).

18.R.K Gupta Proc. 5^{th} Int. conf. on Nuclear Reaction Mechanisms, Varenna, P 416 (1988).

19.S Malik and R K Gupta Phys. Rev. C 39, 1992 (1989).

20.J. Maruhn and W. Greiner, Phys. Rev. Lett. 32, 548 (1974)
21. R.K Gupta, W. Scheid, and W. Greiner, Phys. Rev. Lett. 35, 353 (1975).
22.R.K Gupta and W. Greiner, Heavy Elements and Related New Phenomena, World Scientific, Singapore, edited by W. Greiner and R.K Gupta, Vol. I, P 397; P 536 (1999).
23.D R Saroha and R.K Gupta, J. Phy. G 12, 1265 (1986).
24.S. Kumar and R.K Gupta, Phys. Rev. C 55, 218 (1997).
25.R.K Gupta, M. Balasubramaniam, C. Mazzocchi, M. La Commara, and W. Scheid, Phys. Rev. C 65 024601 (2002).
26.N.J. Davidson, S.S. Hsiao, J. Markram, H.G. Miller, and Y. Tsang, Nucl. Phys. A570, 61C (1994).
27.G. Audi and A.H. Wapstra, Nucl. Phys. A595, 4 (1995).
28. W. Myers and W.J. Swiatecki, Nucl. Phys. A81, 1 (1966).
29. J. Blocki, J. Randrup, W.J. swiatecki, and C.F Tsang, Ann. Phys. (NY) 105, 427 (1977).
30.G. Royer and J. Migner, J. Phy. G 18, 1781 (1992), and earlier references therein.
31.A.S Jensen and J. Damgaard, Nucl. Phys. A203, 578 (1973).
32.H Kroeger and W Scheid, J. Phys. G: Nucl. Phys. 6, L85 (1980).

Chapter 3

REVIEW OF RESULTS AND DISCUSSIONS

REVIEW OF RESULTS AND DISCUSSIONS:-

The mass region A=68-82 is of special importance because majority of nuclei in this mass region are Superdeformed with β_2 as high as 0.5 [3] and therefore are useful in reference to Nuclear synthesis problems. It has been observed that in contrast to the Z(=N) = 40 ^{80}Zr nucleus, the Z = 38 and N = 40 ^{78}Sr nucleus is much more stable against decays via an alpha particle or any other heavy cluster. The calculated cluster-decay half-life times were found to be larger than 10^{100} s for ^{78}Sr as compared with $\approx 10^{50}$ s for ^{80}Zr . This result, though consistent with Q-value considerations and binding energy effects, has an apparent consequence for the stability of the deformed Z = 38 (and also N = 38) shell, which reinforces the N = 38 [4,5] deformed shell to make ^{76}Sr a very stable Superdeformed nucleus in nature. A similar stability of deformed shells against cluster decays is expected in other regions [2] like Z = 38 and N = 60, thereby stressing that cluster decay studies contain information about the organization of nucleons inside the nucleus. Also, this study points to other possibilities, like the cluster radioactivity with deformed daughters and the superheavy elements produced by colliding deformed nuclei.Another set of calculations on ^{76}Sr nucleus show that, in a clear asymmetric mass distribution, ^{76}Sr nucleus allows preferential alpha-nuclei transfer resonances. Thus for obtaining complete fission products, one has perhaps to go to at least double the Coulomb barrier energies. This provides a large center of mass velocity which facilitates the verification of full momentum transfer and easy identification of the fragment's atomic number at higher incident energies. Also, the high energy solution at forward angles should enhance the observation of compound-nucleus decay and virtually eliminate any possible deep inelastic contribution.

Another interesting aspect of nuclei with masses $68 \leq A \leq 82$ having charges $34 \leq Z \leq 40$ (only even–even cases) was studied in [1]. The figure 1 of [1] showing mass fragmentation potential $V(\eta)$ for a few illustrative cases, calculated at the touching configuration $R=C_1+C_2=C_t$ is shown as Fig 3.1 for drawing

comparative fragmentation behavior among the superdeformed nuclear system. It is well established fact that deep potential energy minima are found to occur only at $N = Z$, $A = 4n$ α-nuclei for the α -like parents, whereas the same for other parents occurs both at α - and non-α -like nuclei. This means that $N = Z$, $A = 4n$ parents are expected to decay with higher probability via α -nuclei, but the $A = 4n+2$ parents decay equally well via α - and non- α nuclei.

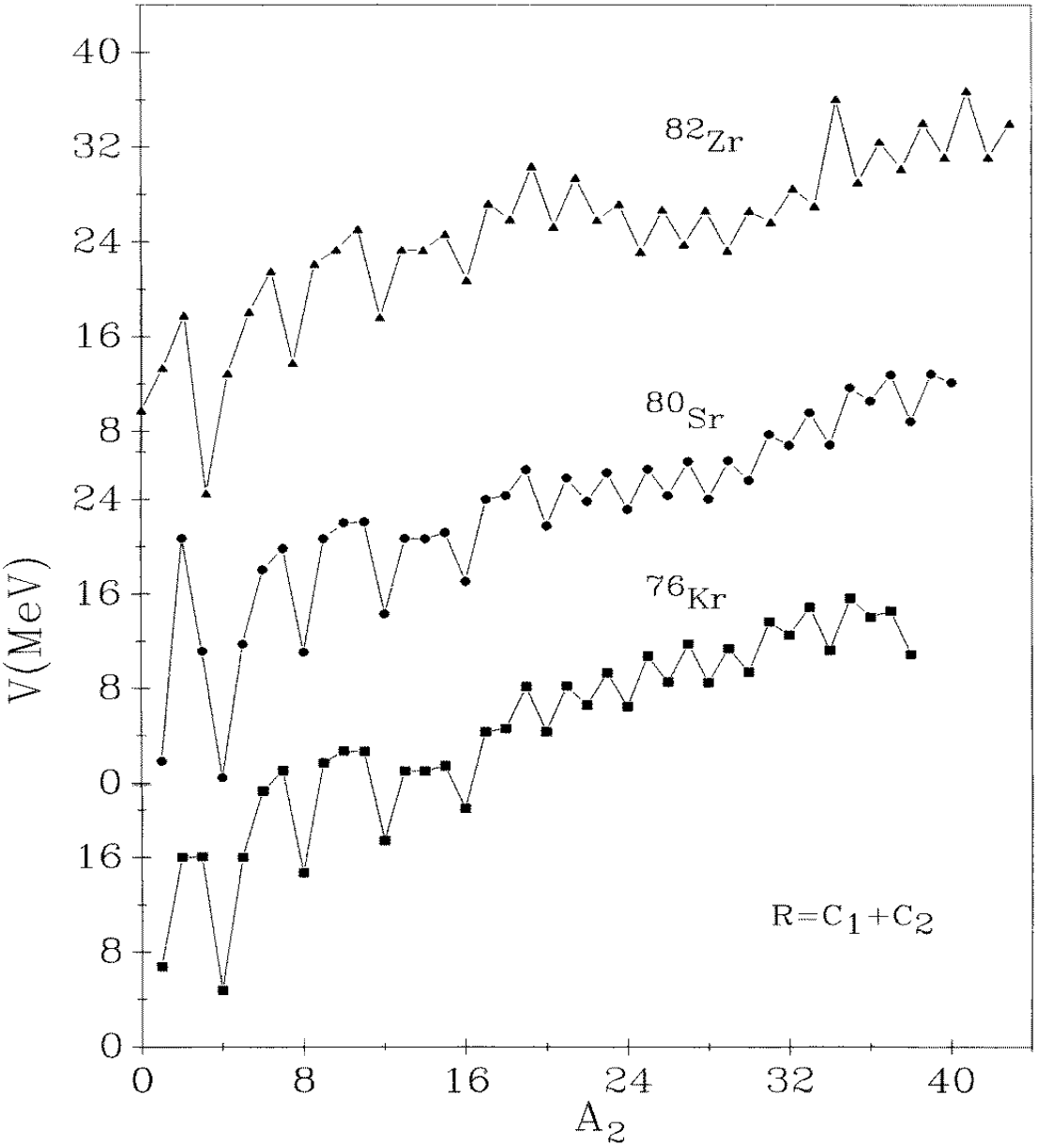

Figure.3.1: Fragmentation Potential for ^{76}Kr, ^{80}Sr and ^{82}Zr taken from [1]

One may clearly see from Figure 3.1 that ^{76}Kr, ^{80}Sr and ^{82}Zr show almost similar fragmentation path showing preferential α-decay structure. Evidently the fragmentation potential for ^{76}Kr and ^{80}Sr is almost identical, where as fragmentation potential of ^{82}Zr shows minor variation especially for larger clusters. The cluster decay studies [1] clearly depict that ^{76}Kr is most stable nucleus among other competing isotopes of Kr, Sr and Zr nuclei. This Figure: 3 of [1] is plotted here as Figure 3.2 for establishing the concept of relative stability of Superdeformed nuclei in this special set of nuclear masses.

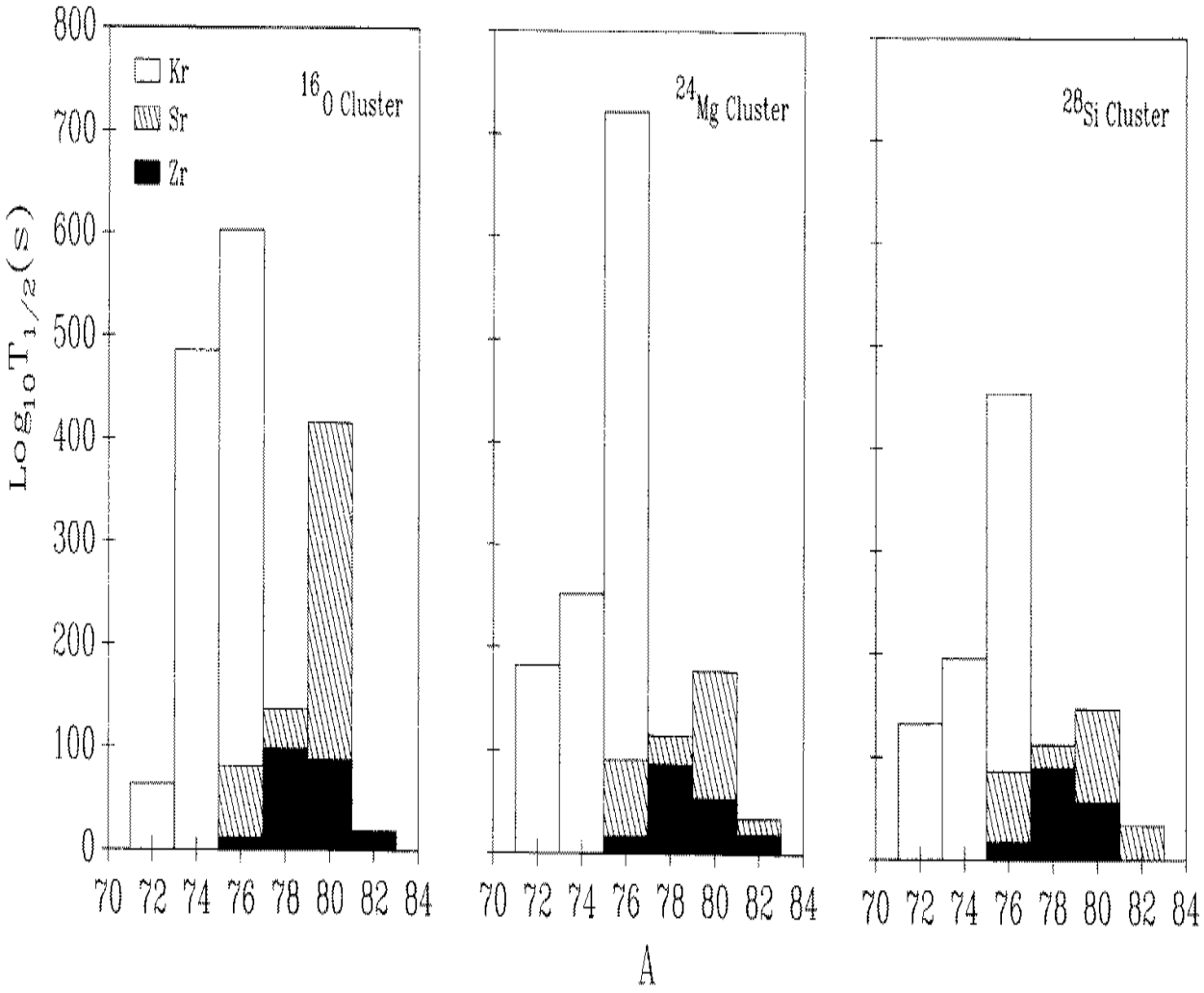

Figure.3.2: Histogram of $\log_{10} T_{1/2}$ (s)-values versus the parent masses for ^{16}O, ^{24}Mg and ^{28}Si cluster decays taken from [1].

The $\log_{10} T_{1/2}$ (s) results shown in Fig 3.2 clearly predict that ^{76}Kr is the most stable nucleus in mass region A=68-82 (Superdeformed region) against various clusterizations. Clearly ^{16}O, ^{24} Mg and ^{28}Si clusters were shown to be most stable. The interesting aspect of these calculations is that with the inclusions for subtraction of neutrons a stable isotope looses its stability significantly.

In terms of shell structure effects, the stability of ^{76}Kr strongly indicates the reinforcing of the stable Z= 36 (deformed) shell with stable N=40 (spherical/deformed) shell. This kind of reinforcing of the deformed stable shells in the spherical/ deformed stable shells could be extremely useful in deciding various target projectile combinations along with its strong applications in the nuclear structure and fusion reaction studies using deformed nuclei.

In order to understand the clusterization of ^{76}Kr we have carried out systematic calculations using Two Center Shell Model. The single particle energies of ^{76}Kr are shown in Figure: 3.3.The basic aim of calculating single particle energies is hat we are interested in calculating the shell gap between highest filled level and first empty level. The shell gap will account for the stability of nucleus against the emitted cluster. In other words if shell gap is more, the stability against anticipated cluster is more or vice versa. λ is fixed at touching configuration with ε at 0.75 in reference to optimization done on the basis of dinuclear system model calculations. The deformation values β_1 and β_2 are varied systematically in order to get optimized shell gap. Here we fixed quadrupole deformation (β_2) of one fragment and vary the β_2 of another fragment so as to maximize the gap between last filled and first empty level. Then we fix the optimized β_2 and vary the β_2 of earlier fragment. We keep on doing β_2 iterations, until we find the maximum shell gap in order to establish stability of concerned nuclear systems.

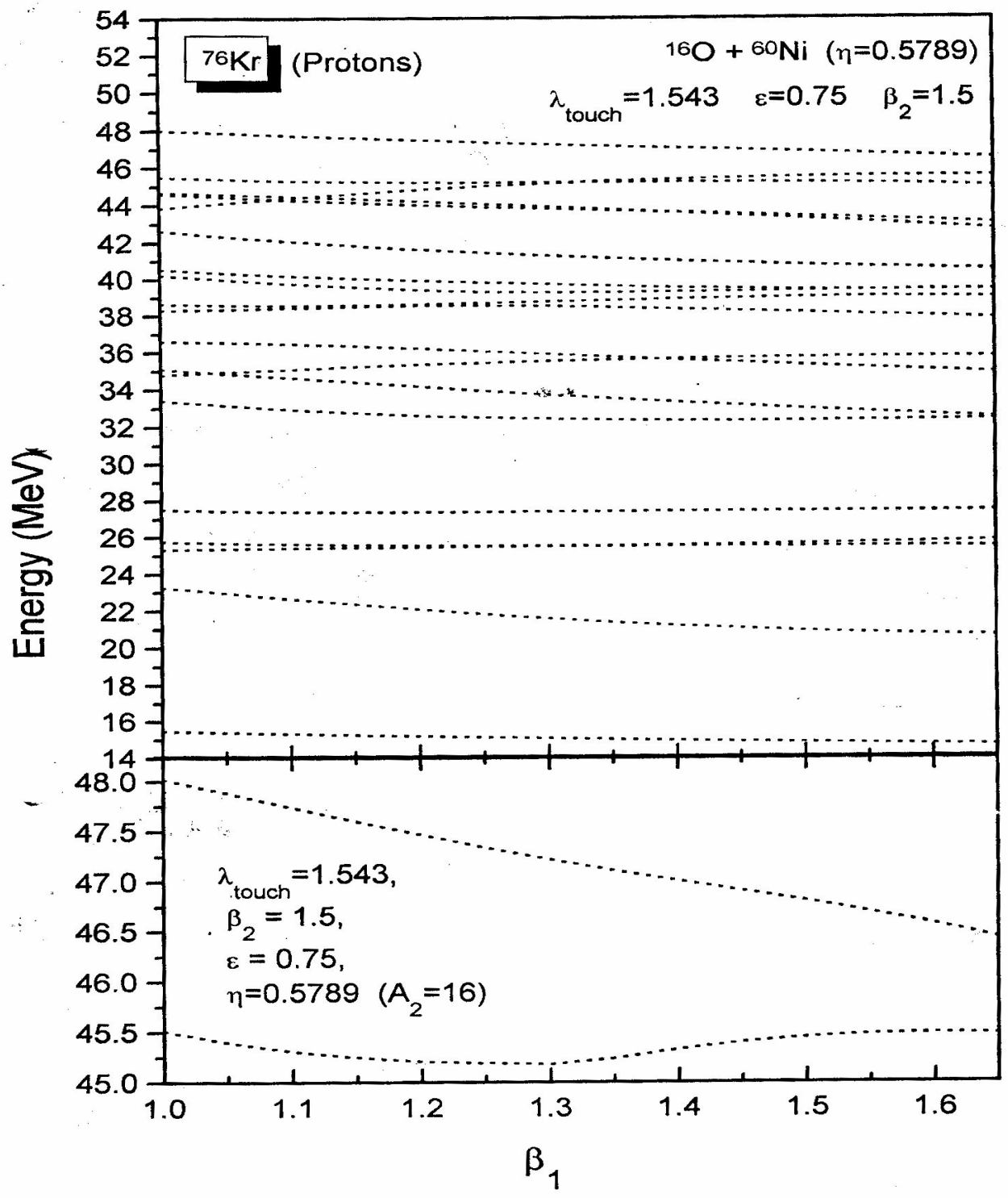

Figure.3.3: Single particle energies as a function of quadrupole deformations.

We have carried out the 4-nucleon clusterization of ^{76}Kr using TCSM and have optimized the shell gap between highest filled and first empty level. The results are summarized in table 3.1. The choice of λ, β, ε etc are mentioned for drawing further inferences, if any.

Table: 3.1 TCSM calculations on showing shell gap for 4-nucleon clusterization of ^{76}Kr.

^{76}Kr						
Cluster(A_2) (A2)	η	λ(touch)	ε	β1	β2	Δ(MAX)
0	0.9999	1.2524	0.75	1.25	1.4	2.01
4	0.8947	1.5323	0.75	1	1.4	1.56
8	0.7895	1.603	0.75	1.55	1.05	2.22
12	0.6842	1.6153	0.75	1.05	1.15	1.81
16	0.5789	1.5427	0.75	1	1.05	3.52
20	0.4734	1.6795	0.75	1	1.05	2.66
24	0.3684	1.7229	0.75	1.6	1.75	2.33
28	0.2632	1.7911	0.75	1.55	1.05	1.08
32	0.1579	1.583	0.75	1	1.45	2.87
36	0.0526	1.5869	0.75	1	1.85	2.63

The figure 3.4 shows variation of shell gap Δ(MAX) as a function of cluster mass for the 4-nucleon clusterization of ^{76}Kr . From figure 3.4 it is clear that shell gap is maximum for ^{16}O fragmentation i.e. our Two Center Shell Model calculations clearly depict that ^{76}Kr is the most stable deformed nuclear system against ^{16}O cluster.

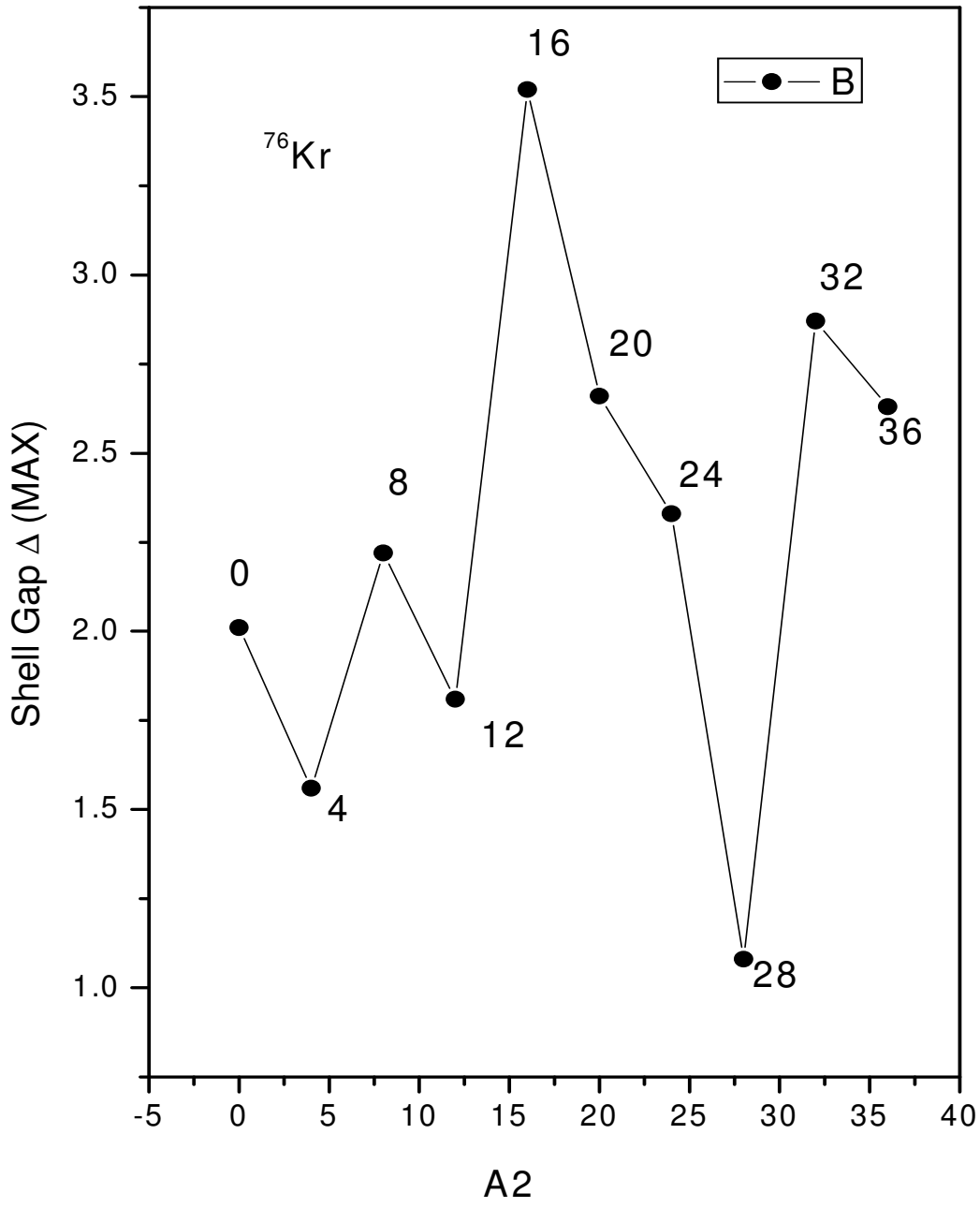

Figure.3.4: Shell gap Δ_{max} for 4-nucleon clusterization of ^{76}Kr as a function of cluster mass.

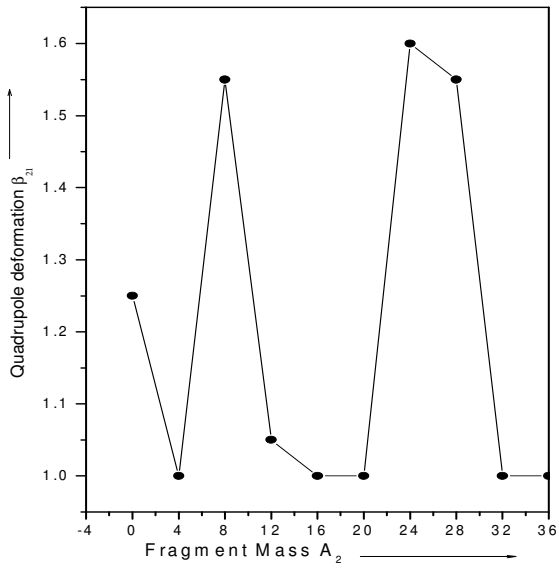

Figure.3.5: Optimized Quadrupole deformation β_{21} as a function of fragment mass.

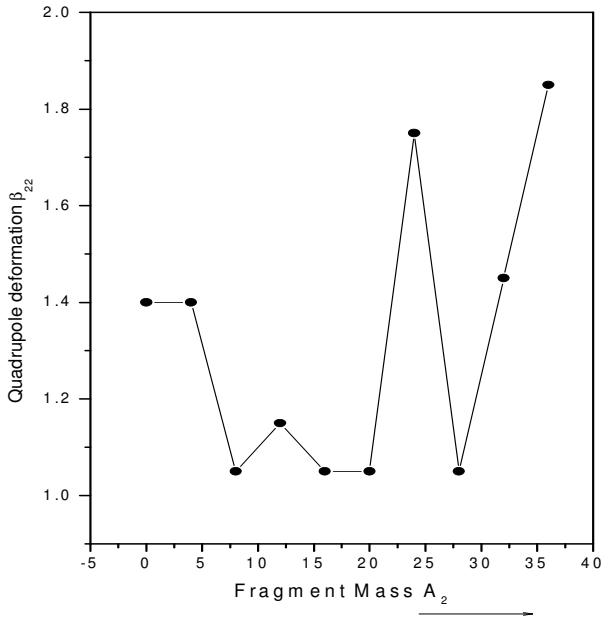

Figure.3.6: Optimized Quadrupole deformation β_{22} as a function of fragment mass.

Figure 3.5 and 3.6 show the variation of optimized quadrupole deformations β_{21} (Fragment) β_{22} (Complementary Fragment) respectively as a function of fragment mass. The optimization of quadrupole deformation is done in order to maximize the shell gap between highest filled level and first empty level using Two Center Shell Model calculations. These optimized quadrupole deformation values could be utilized for future in using equations on concerned nucleus and its decaying fragments.

References

1. Stability and instability of nuclei in the mass region *A* = 68–82based on exotic cluster decay studies J. Phys. G: Nucl. Part. Phys. 25 (1999) 1089–1097.
2. Hamilton I H, Hansen P G and Zganjar E F 1985 Rep. *Prog. Phys.* 48 631
3. Lister C J et al 1987 Phys. Rev. Lett. 59 1270
4. Gupta R K, Scheid W and Greiner W 1991 J. Phys. G: Nucl. Part. Phys. 17 1731
5. Hamilton JH, RamayyaAV,Maguire C F, Piercey R B, Bengtsson R,Moller P,Nix J R, Zhang J-Y, Robinson R L and Frauendorf S 1984 J. Phys. G: Nucl. Phys. 10 L87

Chapter 4

SUMMERY AND CONCLUSION

Summery and Conclusion:

The mass region A=68 to 82 is observed to be an island of superdeformed nuclei having large quadrupole deformations of the order of 0.5. These super deformed nuclei play significant role in various nuclear phenomena including synthesis of heavy/super heavy nuclei. Although all these superdeformed nuclei are important and play significant role in understanding various nuclear properties. But one question is of extreme importance and relevance that among all these super deformed nuclei, which one is most stable against the clusterization process. In other words, its important to investigate the relative stability among these super deformed nuclei so as to draw conclusions and inputs for future experiments planned with such target projectile combinations. Keeping this in mind the stability or instability of these super deformed nuclei is reviewed on the basis of cluster decay calculations. The cluster decay calculations indicate that ^{76}Kr is most stable nucleus among other competing isotopes of Sr and Zr in this special super deformed region. An attempt is made to understand the clusterization of most stable nucleus i.e. ^{76}Kr using Two Center Shell Model calculations. The Interesting fact about deformed/superdeformed nuclei is that when one of the reaction particle is taken as deformed or superdeformed fusion probability gets enhanced. This is because for deformed combinations height of potential barrier gets decline and hence fusion probability goes up. So deformed or superdeformed nuclei are very interesting candidates for the synthesis of Superheavy elements.

Using Two Center Shell model Calculations we have calculated the shell gap for 4-nucleon clusterization of ^{76}Kr. For the calculations we have taken λ at touching configuration and ε=0.75 in reference to dinuclear system model calculations. However quadrupole deformations are optimized by varying β_{21} and β_{22} values in

order to get maximum shell gap between highest filled level and first empty level of the single particle energies calculated using Two Center Shell model. Our calculations clearly depict that ^{76}Kr nuclear system is most stable against ^{16}O cluster followed by A_2 =32 and 36 and 20 fragment mass. These calculations are extremely important and useful to utilize these superdeformed nuclei to understand various nuclear properties along with nuclear synthesis in heavy and superheavy mass region.